OERA Research on Tidal Marine Energy

Application of drifters with suspended hydrophone arrays to assess harbour porpoise use of the water column and spatial overlap with MRE devices in Minas Passage

FINAL TECHNICAL REPORT – 30 April 2019

Submitted by
Brian Sanderson, Mike Adams and Anna Redden
Acadia Centre for Estuarine Research, Acadia University
Nova Scotia, Canada

ACADIA Tidal Energy INSTITUTE

ACADIA ESTUARINE CENTRE FOR RESEARCH

Application of Drifters with Suspended Hydrophone Arrays to Assess Harbour Porpoise Use of the Water Column and Spatial Overlap with MRE Devices in Minas Passage

Brian Sanderson, Mike Adams, and Anna Redden
Acadia University

April 30, 2019

Contents

1 Executive Summary

The harbour porpoise (*Phocoena phocoena*) is by far the most commonly observed marine mammal species in the waters that sweep through and nearby the FORCE in-stream turbine Test Site in Minas Passage. Over the last 10 years, there have been consistent measurements to monitor the activity of harbour porpoise at and near the FORCE Test Site. Those measurements were made with a widely used event detector called the C-POD (Chelonia Ltd) that conveniently detects harbour porpoise vocalizations. A good deal of baseline knowledge has been obtained to date about how porpoise vocal activity varies according to season, tide, and from daylight to nighttime in Minas Passage [1].

Ultimately, it is necessary to understand how harbour porpoise respond to the installation of one or more in-stream tidal turbines. What is required are ways to measure positions of individual porpoises relative to the position of the turbine. Imaging sonar is one possible option but does not usually give fully three dimensional positions. Also, harbour porpoise can detect acoustic transmissions from imaging sonar signals and may well respond to them, thus imaging sonar would not be sufficient in itself.

Our present project uses an array of synchronized hydrophones to not only detect porpoise vocalizations but to also determine where the detected porpoise was located when those vocalizations were made. Our method makes a small number of highly-targeted, high-quality measurements by suspending a hydrophone array beneath a low-cost but high-fidelity drifting platform. Measurements are subject to detailed analysis in order to detect porpoise vocalizations and utilize them for obtaining positional information and for refining mathematical methods of detection. Always, methods focus on performance and automation. Checking performance is critical, and is also semi-automated. The objective is to continuously improve both field and mathematical techniques so that better analysis methods lead to better measurement methods and greater efficiency and effectiveness.

We envision that our measurement and mathematical methods would be most effectively translated for turbine installations from floating platforms. Floating platforms allow experimentation and adaptation, at least in principle. Once perfected on floating platforms, translation to gravity-base platforms may become practicable.

Of more immediate application, our measurements and methods enable a better understanding of the C-POD event detection measurements that have been made over the last 10 years [1]. In addition to the synchronized hydrophone array, many of our drifter measurements included C-POD instruments. The C-POD uses a proprietary algorithm to record properties of detected echolocation events but does not record the sound signal from which events are obtained. Independent detection of porpoise vocalization measured by the synchronized hydrophone array is compared with C-POD detections in order to quantify instrument performance.

2 Introduction

In view of undesirable aspects of reliance on fossil fuels [2, 3, 4, 5] attention has shifted to exploiting renewable energy[1] resources. Hydroelectric dams are the largest source of renewable electric energy generation [6] on the global scale. Similarly, low-head tidal empoundments have been demonstrated effective for generating electricity. Obtaining hydroelectricity from rivers has ecological effects [7, 8, 9] and fish mortality has been associated with the low-head tidal turbine [10] installed at Annapolis Royal.

The Bay of Fundy has the potential to provide a great deal of renewable energy [11] if in-stream tidal turbines are deployed where currents are fast. In-stream tidal turbines operate in open water so pressure forces are greatly reduced from those of low-head installations. Most importantly, marine animals might *avoid* an in-stream turbine because their path is not constrained by a barrage. It is reasonable that in-stream tidal turbines will not be nearly so ecologically disruptive as obtaining hydroelectricity from dammed rivers or tidal empoundments.

The Fundy Ocean Research Centre for Energy (FORCE) has a Test Site in Minas Passage, Bay of Fundy. This site has infrastructure for testing in-stream tidal turbines and their environmental effects. In support of such testing, baseline information has been obtained regarding tidal currents, ambient sound, and marine animals.

One of the outstanding questions for which Canadian legislation [12] needs an answer is:

> *Will marine animals be harmed in some way when they encounter an in-stream tidal turbine?*

Presently, the answer is not known [13]. The broad objective of the present project is to make measurements and develop methods that are required to address the above question, at least for the dominant marine mammal species.

Passive acoustic measurements to detect marine mammal vocalizations at and near the FORCE Test Site have consistently shown presence of Atlantic harbour porpoise (*Phocoena phocoena*) during the last decade [1, 14, 15]. Most of the measurements were made using C-POD (Chelonia Ltd) instruments which log events corresponding to porpoise vocalizations. Such sustained measurement programs indicate how porpoise activity varies seasonally, from daytime to nighttime, and with the tidal cycle. This information is obviously useful but it comes with limitations and uncertainties which we seek to understand and overcome.

The C-POD uses a proprietary algorithm to detect an acoustic event (porpoise echolocation click) within the acoustic signal that it measures. The most fundamental uncertainty arises from the fact a logged event does not have its associated acoustic signal recorded. Porskamp et al., [16] compared C-PODs with icListenHF hydrophones on a bottom platform (the lander platform) and found that C-PODs detected fewer porpoise vocalizations than were obtained from hydrophone records by viewing spectrograms or using an early version of our porpoise click detector. In the following work we co-deploy C-PODs and icListenHF hydrophones on carefully designed drifters. Using our more advanced algorithms, we detect porpoise vocalizations within the acoustic signal measured by the icListenHF hydrophone. In this way, C-POD detection performance can be carefully compared with independently obtained porpoise detections (see §4.3.3) for which pressure measurements are available.

[1]The laws of thermodynamics preclude truly renewable energy but tides and solar will persist on the billion-year time scale. Wind also persists because it is solar powered.

Strong currents in Minas Passage have been associated with poor performance of the C-POD [14, 1]. The most obvious problem is caused by the C-POD buffer filling with non-target acoustic events which causes the instrument to lose recording time. Non-acoustic noise (also called flow noise and pseudo-sound) [17] caused by high-frequency vibrations in fast currents has been considered to be a cause of lost time in C-POD measurements. By using a drifter as our measurement platform, we largely avoid pseudo-sound (see §5.1) and have been able to demonstrate C-POD lost time relative to fast currents increasing ambient sound level as opposed to pseudo-sound [18], §4.3.1. Comparisions of hydrophone measurements made with different instrument mount systems (drifters and rigid bottom platforms) are also made in §4.3.2.

It is important to be able to measure the abundance of harbour porpoise. For example, if measurements showed that abundance reduced at some site after an in-stream turbine was deployed then that might indicate that porpoises avoid the turbine and thereby avoid direct contact. However, event detectors only measure vocalization activity. To measure abundance, one requires additional information. A vertical array of three or more synchronized hydrophones can provide some of that additional information by enabling calculation of the distance to the porpoise and the depth of the porpoise.

We analyse measurements made in 2017 by a vertical array of two synchronized hydrophones attached as a vertical array beneath a drifter. Two hydrophones are not in themselves sufficient to obtain distance and depth. Nevertheless, it is possible to determine whether porpoise are above or below the level of the hydrophone (see §4.4.1) and sometimes reflected clicks can be used to obtain distance to the porpoise and its depth (see §4.4.3).

Harbour porpoise clicks have a narrow beamwidth [19] and this raises the problem of whether or not all of the hydrophones within an extensive array will detect a given porpoise click. This is an important matter to investigate because many detections are required to obtain the position from which the click originated. In §4.4.2 we seek to quantify the probability of detection by a pair of receivers and diagnose additional factors that limit that probability.

Existing literature reports beamwidth of porpoise clicks but little seems to have been documented regarding off-beam click levels. Additional drifter measurements, made in June 2018, used a vertical array of 4 synchronized hydrophones. Such an array enables the depth of the porpoise and its horizontal distance from the array to be estimated whenever a click is received by at least 3 hydrophones. Preliminary results in §5.3 are encouraging and include many instances when porpoises are close to the hydrophone array. Such measurements are expected to be useful for diagnosing whether or not off-beam click levels are sufficient to assist with measuring position of nearby porpoises. Ultimately, this is a matter of considerable importance for designing hydrophone arrays that might obtain three-dimensional tracks of porpoise when (if) they closely approach an instream turbine.

Many additional matters can be addressed in future analyses of the June 2018 measurements. Those matters will be material for a M.Sc. thesis (Mike Adams, Acadia University).

Drifters make measurements in the coordinate system of the moving water. There are advantages to obtaining such measurement, in addition to avoidance of pseudo sound. Harbour porpoise have a typical swimming speed [20] far less than the fast currents at the FORCE Test Site so we can consider the drifter as moving in a similar coordinate system to the porpoise. Detected click trains can be expected to contain more clicks when measurements are made moving with the water than when the measurements are made with a hydrophone that is at a geographically fixed position (see §4.3.2). Similarly, opportunistic detections of a fish carrying

an acoustic tag provided a rough measure of how that fish moved relative to the water motion (see §4.4.4).

The usual difficulty with drifter measurements is that the drifter motion is difficult to predict and often the trajectory strays from the zone where measurements are required. Previous drifter measurements made by Acadia University and Gulf of Maine Institute suggest quasi-stable trajectories through Minas Passage. This might also be anticipated by the observation of converged flotsam in Minas Passage and Channel [21, 22, 23]. In §6 we report on a long duration drifter track that passed back and forth through Minas Passage. Dynamics of the quasi-stable drifter trajectories are explored in §6.3 and additional drifter studies are analysed in an effort to roughly demark neighbouring zones with different classes of drifter trajectories. Experimental measurement confirms our expectations and invites further consideration of drifters as platforms for making environmental measurements for this tidal site (see §6.4).

3 Outline of Project Report

The present project builds on previously obtained measurements. In June 2017, we suspended two synchronized icListenHF hydrophones beneath a drifter and tracked it on 6 days as flood/ebb tides moved it in Minas Channel, Minas Passage and Minas Basin. We also obtained coarse resolution measurements of a satellite-tracked drifter that seemed to indicate trajectories in that region that had long-term stability.

The above measurements motivated our proposal to use drifters fitted with GPS and multiple hydrophones as low-cost, high performance marine mammal monitoring platforms. OERA subsequently funded our Open Call Proposal which provided partial funding for:

Activity 1: Analysis of porpoise detections, and associated observations, made during the June 2017 hydrophone-drifter study (Honours thesis study of Mike Adams, supervised by Redden and Sanderson).

Activity 2: Minas Passage drifter field test with 4 synchronized hydrophones for assessments of porpoise depth in the water column and their detection range (distance from hydrophone).

Activity 3: Deployment of satellite-tracked drifters (location transmitted at < 1 hr intervals) in Minas Passsage and track for many tidal cycles.

This final report documents achievements within three main sections (§4, §5, §6) which respectively correspond to the above three activities.

For the sake of logical completeness, the present report includes results and analyses that go well beyond the original ideas and deliverables of the proposal. A few interesting results will be briefly discussed with references to studies in which the work is more fully reported. We also indicate how our work may be carried forward.

4 Porpoise Detection Analysis

This work utilized hydrophone-drifter measurements that were made previously (June 2017) in Minas Passage. In order to provide a logically complete body of work, we begin by briefly describing those measurements. The work has also been reported in a B.Sc. Honours thesis [24], at the 2018 Marine Renewables Canada Research Forum (three presentations), at the 2018 BoFEP Conference [25], and will shortly appear in two peer-reviewed journal papers [18, 26].

4.1 Drifter-hydrophone measurements: June 2017

Figure 1 shows six drifter trajectories in Minas Passage and adjacent areas. The first deployment (12 June 2017) began at the tail end of the flood tide so the track sweeps from Minas Channel, into Minas Passage, and back into Minas Channel on the ebb tide before being recovered near Cape Spencer. Three drifts (14, 15, 16, June 2017) were made on the flood tide. These first four drifts (1 ebb followed by 3 flood) were on or near a neap tide. Two more ebb-tide drifts (26, 27 June 2017) were completed near the following spring tide.

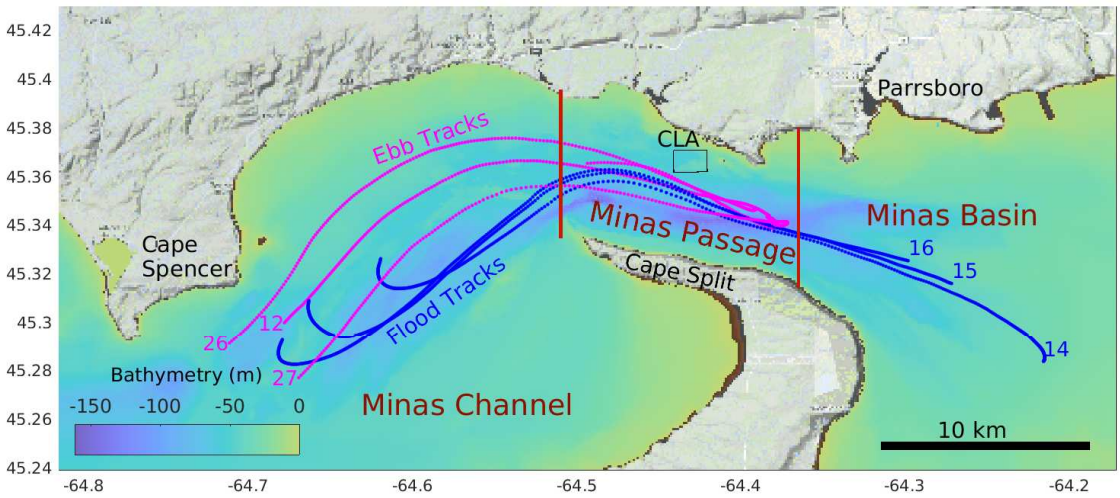

Figure 1: Drifter-hydrophone trajectories on 12, 14, 15, 16, 26, and 27 June 2017. The end of each track is labelled with the day. Trajectories on 14, 15, and 16 of June were obtained on flood tides (blue) which run from Minas Channel to Minas Basin. Trajectories on 12, 26, and 27 June 2017 were on ebb tides (magenta). The FORCE Crown Lease Area (CLA) is marked with a black box. Vertical red lines divide the trajectories into three spatial zones.

The pole-float drifter (Figure 2) used a high-inertia subsurface unit to minimize the influence of lift and drag forces associated with wind waves. The high-inertia subsurface unit consisted of instruments strung along a vertical rope between subsurface flotation and a weight at about 20 m depth. This arrangement suspended instruments along a vertical line. The instrument package included two synchronized icListenHF hydrophones that were 14 and 16 m below sea surface. Synchronization was ±122 nanoseconds of one icListenHF relative to the other (Ocean Sonics Ltd, pers comm, 2017) but deviations from GPS time might have been of the order of seconds. C-PODs were tethered a metre above and below the icListenHF hydrophones. The C-PODs were not synchronized, either to each other or GPS time.

Given that harbour porpoise might interact with the drifter, a GoPro video camera (Hero3 White Edition) was mounted to the drifter at 6.5 m below sea surface. Secchi depths were regularly monitored and were 3.75-4.5 m (mean 4.25 m) during neap tides and 2.75 m during spring tides. Additional tests (12 June 2017) with a Secchi-disk target separated from the GoPro by 2.2 m showed the target to be clearly identifiable for depths 5, 10, 15, and 20 m below the sea surface. Deeper waters were not examined as the camera enclosure was not pressure-rated for testing at greater depths. Juvenile fish were observed in the GoPro images but not harbour porpoise.

Vemco VR2W 69 kHz receivers were included with the instrument layout in order to independently monitor any tagged fish that might pass nearby. No tagged fish were detected. A 69 kHz fish tag was briefly deployed at the beginning of each drift in order to provide a crude time stamp for all instruments.

The drifter was manually deployed from the side of a small (5.5 m) Rigid Hull Inflatable Boat (RHIB). The RHIB drifted, with engine off. Engines were only used to reposition the

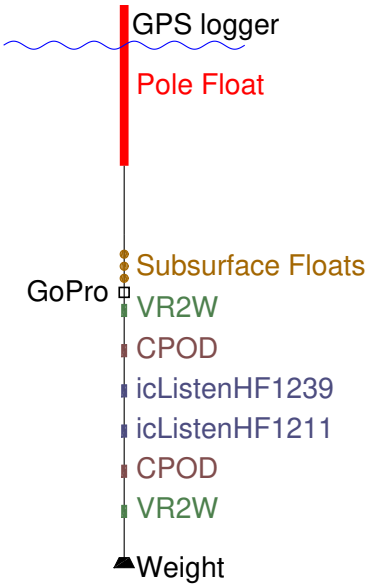

Figure 2: Schematic of the drifter used in June 2017.

RHIB when it drifted more than 800 m from the drifter. The RHIB's 118 kHz echo-sounder was turned off, except for a few brief intervals with total duration 10 minutes. Measurements were in daylight hours with drift durations of 5-7 hours. Positions of the drifter and the boat were logged at 5-second intervals using Garmin GPS units.

The field crew (two scientists and captain) made visual observations throughout all drifts. Harbour porpoise sightings were recorded in the field logbook, noting time, number of individuals, estimated bearing and distance from the RHIB. Occasional seal sightings were also recorded.

An audiovisual representation of the above experiments has been prepared[2]. This presentation shows the key measurements unfolding in an accelerated time frame (3 minutes and 10 seconds for all six drifts). Each visual detection of a harbour porpoise (or seal) is indicated by a line connecting the drifter position to an image. Similarly, operation of the RHIB is illustrated. Detections of harbour porpoise click trains are marked by magenta dots on the drifter trajectories and by an audio signal that corresponds to a single porpoise click that has been slowed by a factor of 40 in order to accommodate the limitations of human hearing.

4.2 Lander platform hydrophone measurements: June 2014

Insights are obtained by comparing drifter-hydrophone measurements with measurements made using other platforms. Hydrophone measurements made on a lander platform have been previously described by Porskamp [15, 16]. An abbreviated description is included here for the convenience of the reader. Two icListenHF hydrophones and two C-PODs were attached to a lander platform as illustrated in Figure 3. The lander platform was deployed at station W1 within the FORCE Crown Lease Area on 5 June 2014 and recovered from Minas Passage on 2 July 2014. Station W1 is located at latitude 45.366220°N and longitude 64.434490°W in about 50 m of water.

[2]The experiments are documented as a movie in a file called movieHRaudio.mp4 which is included with our final submission to OERA.

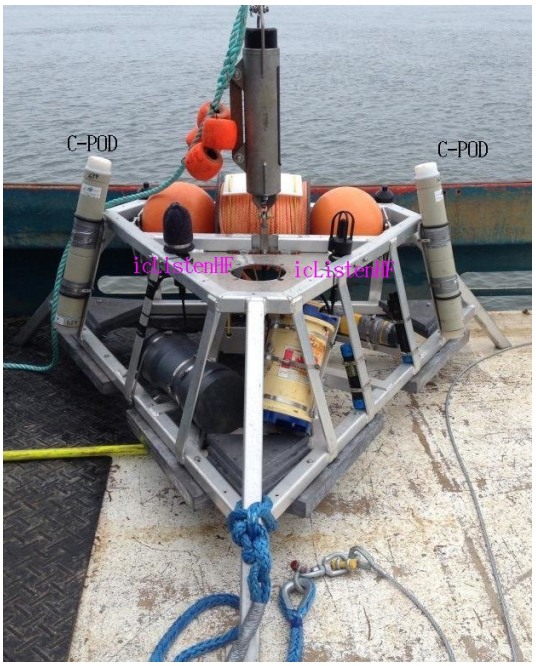

Figure 3: Lander platform with two C-PODs and two icListenHF hydrophones. One icListenHF has a foam shroud over its sensor. Instrument sensors were about 1 m above the seafloor when the lander platform was deployed at the FORCE Crown Lease Area [15].

The lander platform measurements enable comparison of C-PODs with icListenHF hydrophones mounted to a stable platform on the seafloor. Lander-platform C-PODs might also be compared with nearby C-PODs suspended near the bottom using tethered SUB floats. Such comparisons have been previously reported [15, 16, 18]. In particular, it seemed that C-POD detections of harbour porpoise vocalizations were adversely affected when mounted to tethered SUB floats. Such degradation of performance was associated with the instability of tethered SUB floats. Similarly, detection of acoustically tagged fish is degraded when VR2W receivers are mounted to unstable SUB floats in the fast currents of Minas Passage [27].

For this study we have reanalyzed measurements made by the icListenHF SN 1239 which was mounted to the lander platform (shrounded in Figure 3) from 6-20 June 2014. That hydrophone recorded 2 minutes at a high sample rate (512 kHz) every second hour. In total, there were 359 minutes of high sample-rate measurements.

4.3 Coda/icListenHF detections of harbour porpoise

Harbour porpoise (*Phocoena phocoena*) have a distinctive vocalization that takes the form of a high frequency click (Figure 4). The click has pressure fluctuations with frequency typically in the range 124-138 kHz with amplitude modulated with a time scale that is typically in the range 80-150μs. This corresponds to a wavelength of about 0.01 m with the pulse envelope about 0.15 m. A porpoise click has some of its energy focused in a beam. Beamwidth has been measured using a trained, captive animal [19]. For both the vertical and horizontal planes, the beamwidth is about 16^o at the 3 dB level [19]. Click level falls by more than 10 dB at $\pm$20^o from the centre of the beam [19]. Maximum source level for captive porpoise was 172 dB re 1 μPa @ 1 m [19] whereas measurements of wild porpoise gave a source level at the centre of the beam in the range 178-205 dB re 1 μPa @ 1 m [28]. This click is used for navigation and for locating and capturing prey. For the captive porpoise, the interclick interval was typically 20-35 ms longer than the time for sound to make a return trip between the porpoise and target

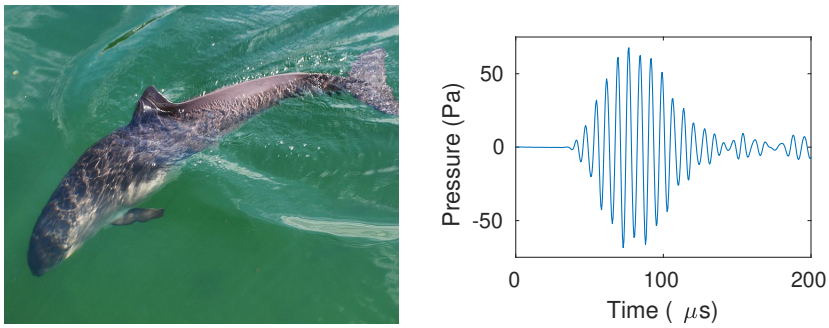

Figure 4: Harbour porpoise (*Phocoena phocoena*) and vocalization (click). Photo by Erik Christensen.

[19].

Coda, a C program developed by Brian Sanderson in partnership with Ocean Sonics Ltd, was used to detect harbour porpoise clicks within icListenHF records. Prior studies have measured clicks by harbour porpoise in Minas Passage and these are used to construct an expected signal shape (response function) for a matched filter. The basic idea is to correlate the response function with hydrophone pressure measurements to detect porpoise clicks. The matched filter is an efficient way to make the calculation. Essentially, the correlation integral is converted to a convolution integral which is efficiently solved using the discrete Fourier transform and convolution theorem [29]. When the matched filter indicates a click may be present, the energy in the frequency band used by porpoises is compared to the energy in the neighbouring bands to reject false-positives caused by broadband noise. A minimum signal level must also be achieved.

Detections obtained directly from Coda applied to icListenHF measurements will be called DCI-detections. For the drifter-hydrophone measurements, 50% of the minutes sampled had at least 4 DCI-detections by one icListenHF or the other. Coda was developed for onboard application within an icListenHF which constrains computational cost and requires that each test for a click is applied, in isolation, to a sequence of 1024 samples. Thus, Coda identifies small segments of data which may be stored and further investigated for porpoise vocalizations.

DCI-detections were further investigated in two stages:

1. An automated application of a more stringent filter on the click level and its ratio to broadband noise and then filtering out DCI-detections that did not belong to a click train. These filtered detections all belong to trains (of at least 3 clicks) and will be denoted FCI-detections so that a FCI-DPM is a minute when either one icListenHF or the other contains FCI-detections. Many DCI-detections were discarded but that still left 19% FCI-DPM. (Detection positive minutes increased to 31% with an alternative approach that selected first for trains and then tested the strongest click in the train relative to broadband noise.)

2. The second stage used semi-automated manual review software to review portions of the time series that contained FCI-detections. The review included: examination of spectrograms, application of the matched filter to 1 s intervals, calculation of click envelopes and regression fits to standard forms, regression fits to obtain click frequency, and consideration of how these things vary within a train of clicks along with evaluations of each click relative to the properties of other types of signal. This manual review did not cause any of the FCI-DPM to be downgraded to detection negative status. However, the manual review did enable us to remove a few questionable clicks (and click trains)

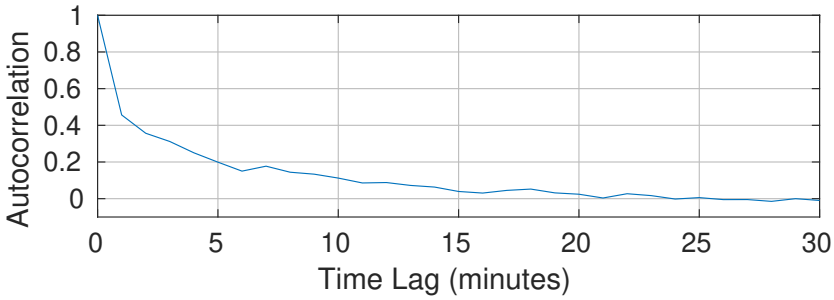

Figure 5: Autocorrelation function for FCI-DPM.

while adding others.

4.3.1 Vocalization activity: time, location, and current

Minutes containing click trains were identified from the C-PODs and icListenHF hydrophones that were attached to the drifter. The six drifter tracks obtained measurements over a total of 1903 minutes. Adams et al. [18] document processing of the C-POD measurements to obtain detections of harbour porpoise click trains. If either of the two C-PODs detected a click train in a minute then that minute was declared to be detection positive, otherwise the minute was set detection negative. Similarly for the two icListenHF hydrophones that had been analyzed using Coda followed by filtering for signal level and reduction of the influence broadband noise followed by selection of only those clicks that belong to a train (FCI-DPM).

The above processing for detection positive minutes gives a sequence of true/false (or 1/0) values for each minute of measurements. This sort of data are "categorical". Many quantities might be estimated from such measurements. Presently we pay particular attention to the proportion p of measured minutes which are detection positive. (Monitoring programs often employ p as a metric that describes harbour porpoise "activity".) If p is obtained from categorical data then a relatively straightforward mathematical derivation gives the following formula for the variance of p

$$\sigma^2 = p(1-p) \tag{1}$$

If each minute is an independent measurement then the standard error of p can be estimated as $\sigma/\sqrt{N}$. Given that the typical swimming speed of a porpoise is about 0.9 m/s [20], it seems likely that if a porpoise is near a drifter during one minute then there is a good chance it will be nearby in subsequent minutes.

We compute time-lagged autocorrelation function for DPM to estimate the time scale over which DPM are not independent (Figure 5). While correlation falls rapidly with lag, there is a degree of correlation that seems to extend out to a period of 20 minutes or more. The integral time scale [30] is the time scale for which measurements of DPM become independent. Integrating the area under the lagged autocorrelation gives an integral time scale of 4 minutes. Thus the standard error (se) of p will be estimated as $2\sigma/\sqrt{N}$.

Table 1 presents the proportion p detection positive minutes for each daytime hour. Thus, if the drifters measured N minutes that belonged to a particular daytime hour (at most $6 \times 60 = 360$ minutes for 6 drifts) then p is the fraction of those N minutes that were detection positive. The proportion of detection positive minutes is low early in the day (1100-1200 UTC) but the number of measurements is small and statistical uncertainty is high. Estimates of p from FCI-DPM do not show any substantive trend during other hours of the day. Estimates of p that are obtained from the C-POD measurements are lower and with high percentage

Hour (UTC)	p, Proportion DPM FCI	C-POD	N	current (m/s)
11	0.012 ± 0.023	0	85	0.58
12	0.084 ± 0.041	0.034 ± 0.027	179	0.69
13	0.19 ± 0.058	0.077 ± 0.04	181	1.3
14	0.19 ± 0.051	0.054 ± 0.029	240	2.2
15	0.28 ± 0.056	0.04 ± 0.025	252	1.9
16	0.2 ± 0.043	0.063 ± 0.026	349	1.7
17	0.17 ± 0.043	0.052 ± 0.025	308	1.9
18	0.21 ± 0.058	0	196	2.6
19	0.21 ± 0.077	0	113	2.3

Table 1: Proportion of detection positive minutes (DPM) in each hour of the day. Note, N is the number of minutes sampled for each hour as obtained from all six drifts.

uncertainty. The present measurements indicate that p might be considered to be roughly constant over the daylight hours which have been best measured.

Figure 1 shows the study area divided into three zones: Minas Channel (MC), Minas Passage (MP), and Minas Basin (MB). The primary consideration of these zones is to separate out the channel-like constraints associated with Minas Passage. Thus, the western end of the MP zone is defined by bathymetry extending a little west of Cape Split, and the eastern extent of MP is defined by where the bathymetry begins to diverge. There is no logically complete way to demark zones without making somewhat arbitrary decisions. For example in Minas Channel, the ebb tide is jet-like whereas drifter trajectories make a convergent loop on the flood tide.

The left panel of Figure 6 shows the proportion DPM in each of the three spatial zones. Proportion detection positive is highest in Minas Passage but not to any substantial extent, as is immediately apparent from the standard errors. The drifter does not randomly sample each zone. Rather, it is deployed so as to be on a trajectory that would place it near Cape Spencer at low tide and in Minas Basin at high tide. Thus, the drifter is moved by faster currents when it is in Minas Passage than when it is in either Minas Channel or Minas Basin, as indicated in the left panel of Figure 6.

Instruments that are deployed on a drifter make measurements by moving with the same water mass. Harbour porpoise typically move slower [20] than currents in the study area [11] so, to a first approximation, drifter-hydrophones might be expected to measure a water mass in which animals remain similarly abundant as they are swept from one zone to another at one time to another. It seems hardly surprising, therefore, that separating our measurements according to time and location does not show some substantial trend.

Proportion DPM does not just depend upon animal abundance, it might also depend upon vocalization activity or performance of our instruments. An aliased effect of current speed could be behind any trends that might be hinted by Table 1 and the left panel of Figure 6.

The right panel of Figure 6 shows proportion detection positive minutes for three broad categories of current speed. It seems that FCI are more likely to detect harbour porpoise vocalizations when current speed is high whereas the C-PODs are more likely to obtain detections when current speed is low. The standard errors are sufficiently large to make us somewhat circumspect and suspicious of aliasing by other unresolved factors. Adams et al. [18] make a

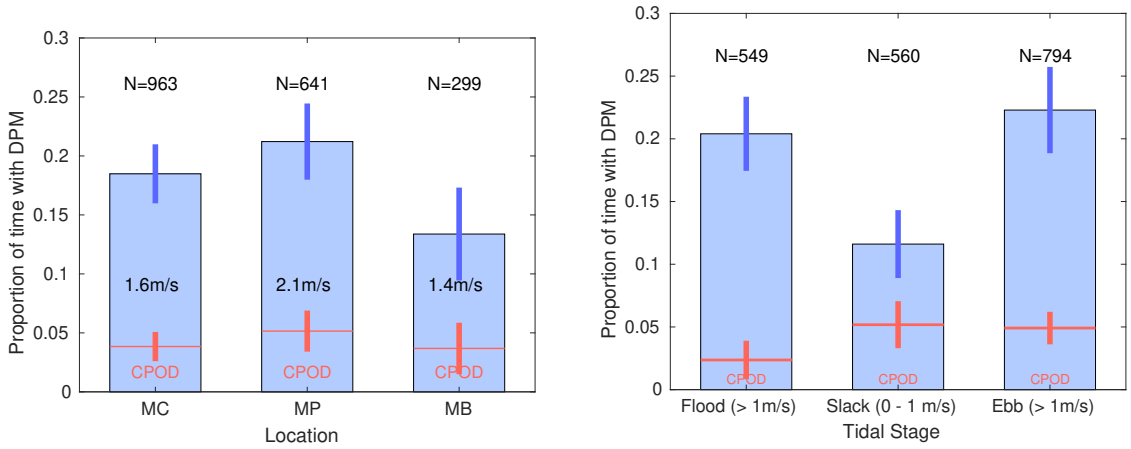

Figure 6: LEFT: proportion of detection positive minutes p for each zone: MC (Minas Channel), MP (Minas Passage), and MB (Minas Basin). The number of measurement minutes N is indicated for each zone. Vertical lines show the standard error. Bars are results ontained from FCI-DPM and the orange lines from C-POD measurements. RIGHT: proportion of detection positive minutes p grouped according to current speed.

strong case for C-POD detection efficiency dropping in fast currents. Our extensive manual review of the FCI-DPM seems to preclude the increase of FCI detections in fast currents being caused by ambient noise that causes "false positives".

The most obvious result from Figure 6 is that the C-PODs have fewer detection positive minutes than FCI-DPM. This matter has been examined in some detail by Adams et al., [18] and we will also consider it briefly in §4.3.3.

Field observations extended to recording anthropogenic activity while measurements were being made. All observed activity could be reasonably considered to be intermittent from the frame of reference of a porpoise. Statistical comparison indicated no credible relationship between intermittent anthropogenic activity and acoustic detections of porpoise activity [24]. This result should not be interpreted as indicating anything about the possible effects that persistent human activity might have on porpoise.

4.3.2 Comparison of drifter and lander platform measurements

Our drifter-hydrophone measurements are made three years after those made using the lander platform, but both sets of measurements are made in the month of June which is the annual peak [1] of porpoise vocalization activity. Also, both sets of measurements use the same icListenHF hydrophones, so that also invites comparison.

The analysis of drifter-hydrophone measurements, above, indicated no meaningful difference in DPM depending upon drifter location, current speed, and day-light hour of the day. This is, perhaps, not surprising given that the drifters follow essentially the same water mass. On the other hand, different water masses flow past the lander platform in the course of the tidal cycle. Measurements on the lander platform also span the day-night hours.

Detections obtained directly from Coda and icListenHF measurements (DCI) are compared in Table 2. The proportion p of DCI detection positive minutes (DCI-DPM) is 62-64% for icListenHF hydrophones mounted to the drifter but increases dramatically to 98% for the

icListenHF Serial No.	Platform	# Minutes sampled	p, se (DCI-DPM)	DCI-detections per DCI-DPM
1211	Drifter	1903	0.62, 0.01	21.3
1239	Drifter	1903	0.64, 0.01	26.5
1239	Lander	359	0.98, 0.01	11.3

Table 2: Detections by direct application of Coda to measurements from each icListenHF deployment. Here, p is the proportion of DCI-DPM and se is an estimate of standard error.

icListenHF Serial No.	Platform	# Minutes sampled	p, se (FCI-DPM)	# Trains/FCI-DPM
1211	Drifter	1903	0.14, 0.01	3.99
1239	Drifter	1903	0.16, 0.01	4.15
1239	Lander	359	0.14, 0.02	1.67

Table 3: Click trains and FCI detection positive minutes.

hydrophone mounted to the lander platform. Perhaps this is not surprising, for a number of reasons:

1. The FORCE CLA seems to have higher ambient sound levels near the frequency band used by porpoise than other locations in Minas Passage [27].

2. Drifter measurements also sample locations in Minas Channel and Minas Basin, where ambient sound is lower than at the CLA. (Sanderson, unpublished analysis).

3. The hydrophone on the stationary lander platform may be affected by pseudo-sound (flow noise) [17].

Increased ambient noise is expected to be associated with increased risk of false detections by Coda. We note, however, that the average number of DCI-detections per DCI-DPM is substantially less for the instrument that was mounted to the lander platform.

One way to screen out spurious detections is to reject them if they are not a part of a click train. Thus, we calculate FCI-detections and FCI-DPM for each set of measurements. This process was followed by a semi-automated review, which did not change detection positive minutes but did enable the click trains to be made more complete (filling in weaker clicks which Coda had rejected but were obviously present when viewed in context).

Interestingly, Table 3 shows that the proportion of DCI-DPM is essentially the same for each set of measurements. On the other hand, detection positive minutes contain many more click trains when the icListenHF hydrophone is mounted on a drifter than they do when mounted to the lander platform.

Drifters move in the coordinate system of the porpoise — that is to say, with the water. Porpoise swimming speed is typically < 1 m/s [20] which is much slower than the tidal currents in Minas Passage. Thus, to a first approximation porpoises are advected to and fro by the tide.

Hydrophones on the drifter sample the same volume of water for a long time, during which time porpoises might slowly meander through that volume. On the other hand, an entirely new volume of water is swept past the lander platform every few minutes when the tide runs

fast. For example, consider that the hydrophone can detect a porpoise out to a range of 300 m. Thus, the length scale of the volume sampled is 600 m and a 3 m/s current will sweep water through that distance in 200 s (less than 4 minutes).

The number of trains in a detection positive minute (right column of Table 3) depends, therefore, upon the coordinate system in which measurements are made. For a given sampling interval, a platform fixed to the bottom will sample more porpoises than a drifter which moves with the water. On the other hand, the drifter will be expected to detect a porpoise over a longer period of time. Thus, if we were to display results as detection positive 10-second intervals then a hydrophone on a lander platform may not appear to be as effective as a hydrophone on a drifter for detecting vocalizations by harbour porpoises.

The semi-automated manual review enables porpoise click trains to be more accurately populated with clicks. Thus it becomes reasonable to consider the interclick interval (ICI). Figure 7 plots the probability density function (PDF) for ICI. The interval between clicks varies over a great range and so the probability density function is displayed with two views. The top view illuminates the PDF for larger values of the ICI but fails to resolve small ICI. Measurements from the drifter show a minima near 0.01 s with a maxima at about 0.035 s with still quite a large number of ICI around 0.1 s. Sound travels a round-trip distance of about 150 m (twice the typical water depth) in 0.1 s, consistent with navigation relative to the bottom. The peak at 0.03 s corresponds to a round-trip distance of about 40 m, perhaps consistent with surveillance for prey. We might imagine ICI larger than 0.01 s as being related to "surveillance" and "navigation". At the lander platform, the PDF diminishes more quickly with respect to ICI, perhaps because water depth is only about 50 m.

The lower plots in Figure 7 suggest two other peaks in the PDF at shorter ICI. Thus we define ICI from 0.001-0.01 s as exploration of a prey target and ICI less than 0.001 s as a feeding buzz.

With regards to the PDF of ICI, the hydrophones on the drifter show some similarity with the hydrophone on the lander platform, but there may also be substantive differences. The three categories of click train for the two hydrophones on the drifter — that are associated with three local maxima in the PDF — roughly translates to the hydrophone on the lander platform. Further, the occurrence of click trains is similar when normalized by measurement time, although the statistics of small mumbers suggests that we should be cautious about this observation. But the distribution of trains between exploration and navigation categories is quite different on the lander platform from that on the drifter (Table 4).

Navigation trains are far more common than exploration trains for measurements made from the drifter whereas the likelihood of exploration and navigation trains is quite similar for measurements made from the lander platform. The difference between measurement methods is stark so we undertake further analysis. The Lander Platform measurements of click trains were examined separately for nighttime and daylight hours. When lander platform measurements are separated according to daylight and nighttime categories (Table 4) we find that the navigation trains become more common during daylight and exploration trains become more common at nighttime.

In early June there are about 8.5 hours from sunset to sunrise. Thus we define the other 15.5 hours as being daylight. Thus we can calculate the number of trains detected per hour of measurement during daylight and nighttime. Table 4 shows that lander platform measurements obtain about four times as many exploration trains per hour at nighttime as during daylight. On the other hand, navigation trains are observed from the lander platform at

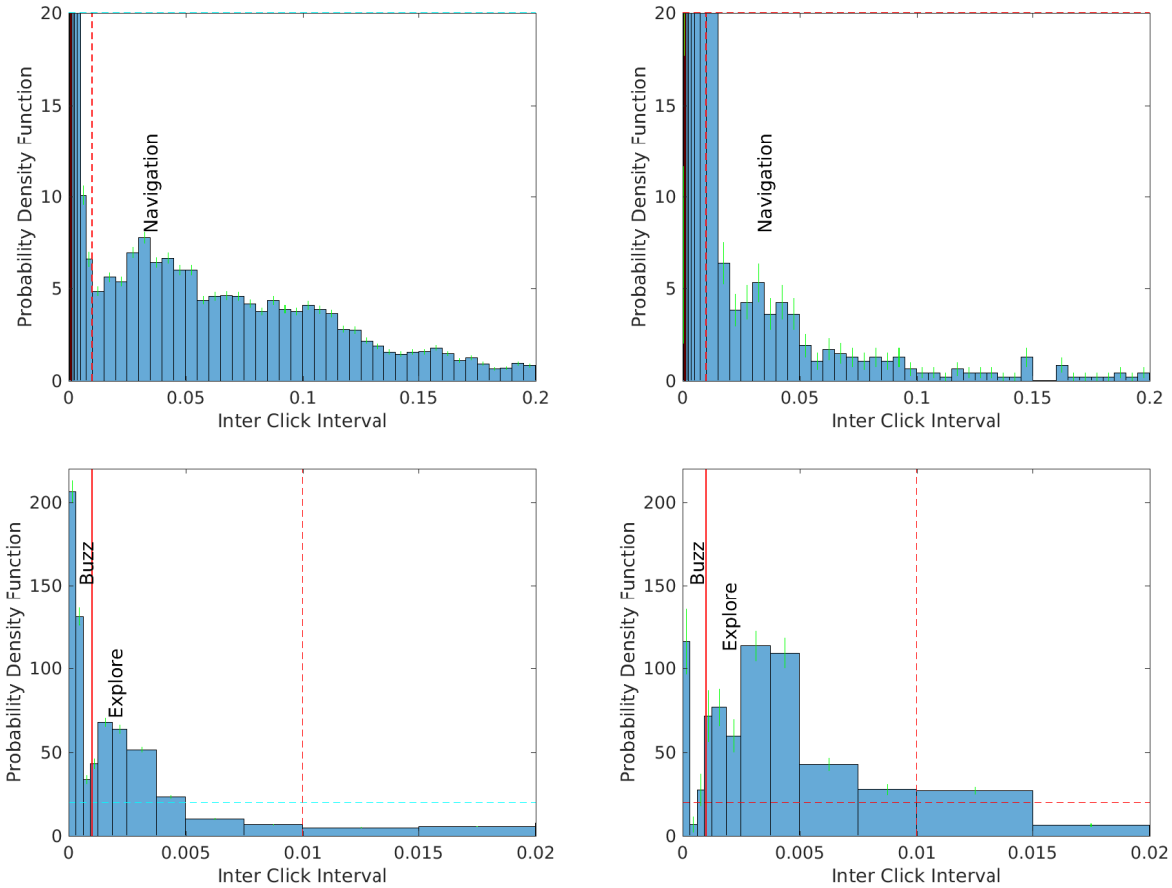

Figure 7: Probability density functions for inter-click interval (ICI). Left: icListenHF hydrophones on the drifter. Right: icListenHF hydrophone on the Lander Platform.

icListenHF Serial No.	Platform	Train Type	# Trains	% of Trains
1211	Drifter	Feeding Buzz	3	0.97
		Exploration	15	4.85
		Navigation	291	94
		Total	309 trains, 121 DPM, 1903 minutes measured	
1239	Drifter	Feeding Buzz	5	1.5
		Exploration	16	4.7
		Navigation	321	94
		Total	342 trains, 133 DPM, 1903 minutes measured	
1239	Lander	Feeding Buzz	1 [0 daylight, 1 night]	2 [0 4]
		Exploration	25 [9 daylight, 16 night]	51 [37 64]
		Navigation	23 [15 daylight, 8 night]	47 [62 32]
		Total	49 trains, 34 DPM, 395 minutes measured	

Table 4: Train types as obtained from icListenHF hydrophones deployed on different platforms. The drifter platform was only deployed during daylight hours. Measurements were made from the Lander platform during daylight and at nighttime.

Train Type	Time	# Trains		Trains/hour-sampled	
		Lander	Drifter	Lander	Drifter
Feeding Buzz	Daylight	0	8	0.00	0.13
	Nightime	1	—	0.50	—
Exploration	Daylight	9	31	2.25	0.49
	Nightime	16	—	8.07	—
Navigation	Daylight	15	612	3.75	9.64
	Nightime	8	—	4.03	—
All Trains	Daylight	24	651	6.00	10.3
	Nightime	25	—	12.6	—

Table 5: Daylight and nighttime variation of the rate of occurrence of train types. The drifter measurements were only made during daylight.

nearly the same rate (trains/hour) during daylight as during nighttime. A higher train rate at night might indicate more feeding than during the day. Perhaps it makes sense that an animal endowed with biosonar might achieve some advantage over visual prey at nighttime. But other reasons have also been suggested for shorter ICI. Above, we note that the lander platform is in relatively shallow water compared to the drifter so signal return time from the bottom is reduced. Also, there has been a suggestion that click trains with progressively increased repetition rate of clicks might be a sign of aggression [31, 32, 33].

4.3.3 Comparing Coda/icListenHF detections with the C-POD and visual observations

Sarnocinska et al., [34] found fewer detections of harbour porpoise vocalizations by C-PODs than by using broadband hydrophones and PAMGUARD marine mammal detection software (Scottish Oceans Institute, Scotland). Others have made similar comparisons of C-PODs with broadband hydrophone measurements and found that C-PODs have lower detection efficiency of harbour porpoises [35, 36] and for bottlenose dolphins [37, 38].

With deployments of our drifter hydrophone-array (Figure 2) we have made concurrent observations of harbour porpoises in three ways. In principle, the C-PODs and icListenHF hydrophones make almost the same measurement with regards to detecting a vocalization by a harbour porpoise. The only difference being that one C-POD is 1 m above the upper icListenHF whereas the other C-POD is 1 m below the lower icListenHF. Given that the 3 dB beamwidth of a porpoise click is 16º, we might expect that a C-POD and its adjacent icListenHF might measure almost the same signal. On the other hand, signal transmission through strongly turbulent flows and interference with reflections (or other signals) can cause localized variation. Nevertheless, direct comparison of detections of many porpoise clicks provides a valid comparison of the efficacy of C-PODs and icListenHF hydrophones.

Visual sightings were made by the three observers in the drifting RHIB which was always in attendance of the drifter. The quiet of the drifting boat assisted visual observation of porpoise because sometimes observers were alerted to the presence of a porpoise by the sound of its blow which guided visual detection. Sightings require an observer to be looking in a direction where a harbour porpoise briefly rolls to the surface. Obviously, the visual sighting of a porpoise need not correspond with a vocalization directed at the C-PODs and icListenHF hydrophones. Also,

sightings of harbour porpoise become much more difficult as sea-state worsens [39]. Timing of drifter-hydrophone experiments was biased towards calm days; nevertheless, sometimes wave conditions made it difficult to spot porpoises. This is particularly the case near Cape Split, where strong currents disturb the sea surface and fewer sightings of harbour porpoises were obtained [24, 18].

One-to-one correspondence of visual observation with acoustic detection cannot be expected but visual sighting does indicate that a porpoise is nearby the drifter and might therefore be detected by the acoustic instruments at some time before or after the sighting. Visual sightings are, therefore, extended with respect to time. Thus, if a porpoise is sighted at some time t then we will say that the minutes from $t - \tau$ to $t + \tau$ are visual detection positive minutes (Visual-DPM). Specification of τ is arbitrary, but it should relate in some physical way to the amount of time that a porpoise might be in the vicinity of the drifter-hydrophone. At a swimming speed of 1 m/s [20], a porpoise travels $2 \times \tau$ m during our extended interval of time. With $\tau = 5$ minutes, this amounts to travelling 600 m which seems reasonable. Our findings are not particularly sensitive to the precise value of τ.

We defined the 5 minutes before and after each sighting to be visual detection positive minutes (V5-DPM). With this manipulation, porpoise sightings might be compared to acoustic detection of porpoise click trains. Figure 8 graphically presents each detection positive minute for each drift (12, 14, 15, 16, 26, 27 June 2017) as obtained for each measurement method. Minutes with detections are plotted with a colored dot. Color indicates measurement method. The resolution of the vector graphics is sufficient to enable each minute to be resolved for each instrument. FCI-DPM are more common than CPOD-DPM. With one exception (around minute 200 of 12 June 2017), CPOD-DPM are always associated with neighbouring or concurrent FCI-DPM. Conversely, there are substantial intervals of time (the latter parts of drifts on 12, 14, 27 June, for example) when FCI-DPM have no associated CPOD-DPM, although there are associated V5-DPM. There seems to be a strong association of FCI-DPM with V5-DPM. It is noteworthy that DPM obtained by acoustic methods are "gappy". It can hardly be expected that a harbour porpoise would direct its narrow beam vocalization towards the hydrophone for many consecutive minutes. Visual sightings are really far more "gappy" but we have artificially extended each sighting over many minutes, as discussed above. The gappy nature of the data makes it unlikely that all three methods will classify a minute as being detection positive (magenta dots in Figure 8).

For mathematical convenience, we will assign the following symbols for the sequences of detections that have all been reduced to a common detection interval:

- I for FCI-DPM (Coda/icListen)
- C for CPOD-DPM
- V for V5-DPM

For the present analysis we concatenate minutes of all six drift experiments. Thus, I, C, V are each a sequence of 1903 logical values with a true value indicating a detection positive minute and a false value when there are no detections in that minute.

The proportion of minutes for which the C-POD obtains detections is the number of true values in C divided by the total number of minutes sampled. This proportion is designated $p(C)$ and is also the probability that the C-POD measures a detection positive minute during

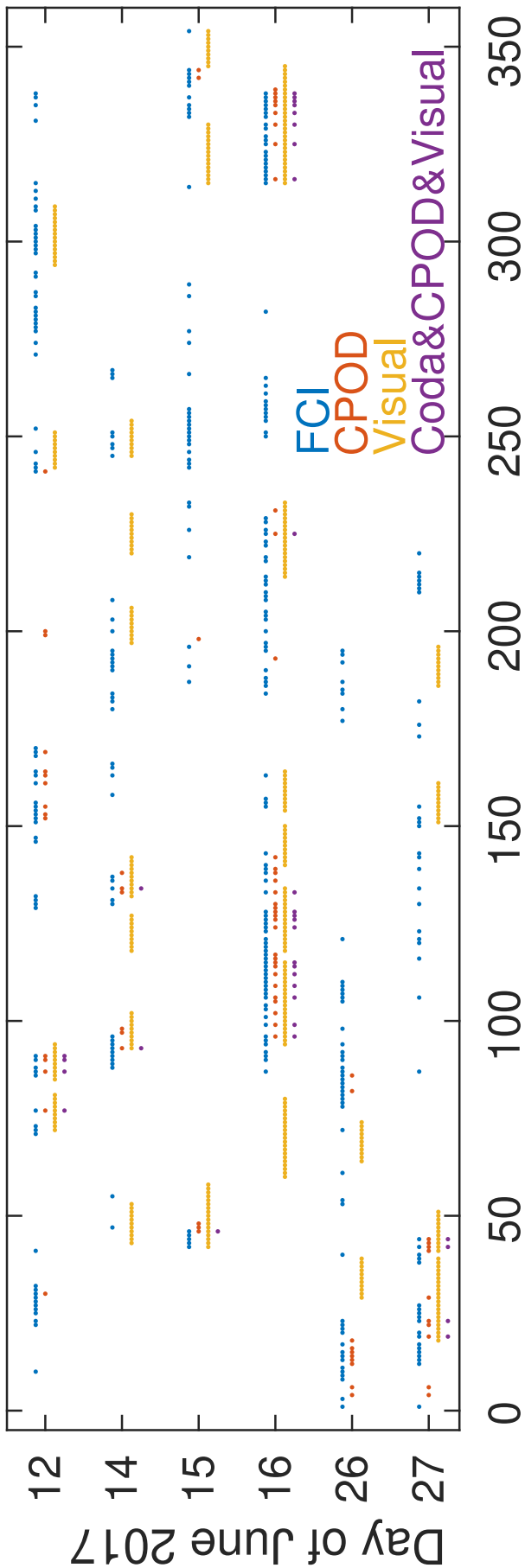

Figure 8: Detections as represented by the sequences of detection positive minutes obtained for: FCI (Coda-icListen), C-POD, Visual observations, and all three methods. The reader can use a vector-graphics viewer to zoom in and resolve individual minutes.

Conditional Probability	$p\pm$SE	Conditional Probability	$p\pm$SE
$p(I\|C)$	0.65 ± 0.05	$p(I\|\neg C)$	0.17 ± 0.009
$p(I\|V)$	0.33 ± 0.02	$p(I\|\neg V)$	0.15 ± 0.009
$p(C\|I)$	0.15 ± 0.02	$p(C\|\neg I)$	0.018 ± 0.003
$p(C\|V)$	0.13 ± 0.02	$p(C\|\neg V)$	0.021 ± 0.003
$p(V\|I)$	0.34 ± 0.03	$p(V\|\neg I)$	0.16 ± 0.009
$p(V\|C)$	0.60 ± 0.05	$p(V\|\neg C)$	0.18 ± 0.009

Table 6: Conditional probabilities of detection obtained from: I for FCI-DPM (Coda/icListen), C for CPOD-DPM, and V for V5-DPM as calculated from visual observations. $p(I|C)$ is the probability that Coda/icListen measures a minute as detection positive given that minute has already been measured detection positive by a C-POD. $p(I|\neg C)$ is the probability given that the minute was not measured as detection positive by a C-POD.

our 2017 experiments. Similarly, the probability of a FCI-DPM is $p(I)$ and the probability of a V5-DPM is $p(V)$.

Figure 8 seems to indicate that the three detection methods are related. To quantify the relationship between I and C we can consider the probability $p(C\&I)$ that both methods obtain a DPM. (Here we have used & to represent the logical "and" operator.) If $p(C\&I) = p(C) \times p(I)$ then we would conclude that I and C are unrelated. On the other hand, if $p(C\&I) > p(C) \times p(I)$ then a true value of I is likely to be associated with a true value of C. It is also possible that $p(C\&I) < p(C) \times p(I)$, in which case C-POD detections become less likely when there are FCI detections.

Adams et al., [18] find that $p(C\&I) \approx 3.5 \times p(C) \times p(I)$ so there is a clear relationship between the CPOD-DPM and FCI-DPM. Similarly, harbour porpoise sightings were related to the acoustic detection of vocalizations.

The relationship between I and C can also be expressed in terms of conditional probabilities. The probability that I will be true for all those elements for which C is true can be written $p(I|C)$. If C-PODs are useful for predicting FCI-DPM then the conditional probability $p(I|C) > p(I)$. Similarly, if the C-POD indicates that no porpoise are present then we would hope that $p(I|\neg C) < p(I)$. Here, the negation operator $\neg$ turns true elements false and false elements true. If both methods of measurement were perfect (and both instruments perfectly co-located) then I and C would be the same so $p(I|C) = 1$ and $p(I|\neg C) = 0$.

Conditional probabilities are presented in Table 6. In every case, it is clear that one method of measuring DPM favourably conditions the probability of obtaining DPM by the other. The association between the two acoustic methods is, however, less than ideal. If both methods worked perfectly, we would expect $p(I|C) = p(C|I) = 1$ and $p(I|\neg C) = p(C|\neg I = 0$. So which is the better method and which is worse?

The result $p(I|C) \gg p(C|I)$ is consistent with the C-POD missing many of the porpoise vocalizations that are detected by FCI (icListenHF hydrophones and Coda). The proportion is $p(I) = 0.19 \pm 0.009$ for FCI whereas it is only $p(C) = 0.043 \pm 0.005$ for the C-PODs.

The FCI method obtained 354 detection positive minutes out of the 1903 minutes measured. Each porpoise vocalization in those FCI-DPM was carefully scrutinized by viewing and analyzing the recorded time series of pressure measurements.

In contrast, C-PODs obtained 81 detection positive minutes out of the 1903 minutes measured. There were 301 DPM obtained by FCI but not obtained by C-PODs. Thus, it seems

that C-PODs have a false-negative problem[3]. But we should hasten to add that the FCI method might also have a false negative problem. The FCI method selects DCI by applying a stringent signal to noise filter and then searching the remaining clicks to find trains of 3 or more. Modifying the method by first searching for trains and then applying the signal to noise filter to the strongest click in the train gave 586 detection positive minutes. The modified method (MCI) puts more emphasis on context and our most recent work (following from the present project) indicates that this is justified.

Of more concern are the 28 C-POD detection positive minutes that were not obtained by the FCI method. There were also 23 C-POD detection positive minutes that were not obtained by MCI (modified method). We used Audacity to carefully review spectrograms and filtered time series of icListenHF measurements made during each of those 23 minutes. Weak porpoise clicks were evident in 10 of those 23 minutes. The Coda algorithm had rejected 3 of them outright and the other 7 were rejected by FCI and MCI filtering. Signals that we interpreted as broadband spikes might have been classified as harbour porpoise clicks for 4 of those 23 minutes. We could find nothing in 4 of those 23 minutes that indicated anything remotely like a porpoise vocalization. Care must be taken, however, because the C-PODs were not synchronized with each other, nor with the icListenHF hydrophones, so the minutes that we viewed in the icListenHF records may not exactly match up with the minutes that C-PODs measured. There was 1 minute when it seemed that the C-POD had classified pings from a 118 kHz echo sounder as porpoise vocalizations. Finally, there were 4 minutes when a 69 kHz Vemco fish tag was evident. Spectrograms showed that the fish tag had a strong harmonic which likely caused the C-PODs to give detection positive minutes in error.

Certainly, C-PODs miss many detection positive minutes. Adams et al., [18] show that C-PODs suffer lost measurement time when current speeds are greater than 1.5 m/s. This seems to be caused by ambient sound causing memory buffer to become filled. Lost measurement time can only account, however, for a small part of the difference between C-DPM and FCI-DPM. Although FCI obtain far more detection positive minutes, they also fail to detect every porpoise vocalization.

The FCI-DPM back up the majority of those minutes that C-PODs classify as detection positive. Some of the false positives were caused by our measurement methods (briefly turning on the echo sounder and briefly deploying a fish tag at the start of each drift) and such things may not be an issue for many C-POD applications. Mostly, we can be reasonably assured (say 80% confident) that a minute is detection positive if a C-POD "says" that it is.

C-PODs have been widely used for environmental effects monitoring in Minas Passage. There are many reasons to suspect that C-PODs suffer from false-negative errors. Presently we show that C-PODs fail to detect many vocalizations that are achieved by icListenHF hydrophones in combination with Coda and review software. Others raise problems associated with lost time [18, 1] and performance issues associated with the instability of tethered SUB floats [27].

Regardless of such difficulties, it is our opinion that C-PODs are valuable for long term environmental monitoring that has been required for compliance with the Fisheries Act [12]. When the objective is to compare long term changes in DPM, it matters little if only some proportion of porpoise vocalizations are detected, just so long as that proportion remains

[3]In part, this might due to the icListenHF hydrophone having greater sensitivity, lower self noise, and bandwidth extending to higher frequencies than the C-POD. If so, then the icListenHF might be able to detect porpoises at a greater range.

stable over time. C-PODs have the advantage of being easy to deploy for relatively long periods of time and being highly automated.

Presently, the icListenHF hydrophone needs to be cabled for long deployments in order to provide power and archive broadband measurements. In principle, when cabled, the icListenHF in combination with onshore processing would be a powerful and convenient method for environmental monitoring. In practice, the methods to conveniently achieve that are still not fully developed. The motivation for the necessary development is not, however, to make a system that achieves the same objective as C-PODs.

Rather, the objective of a system based on Coda detection of porpoises from many synchronized icListenHF hydrophones is to be able to measure the source position of a vocalizing porpoise. The reasons for such measurements are many. Measuring position enables better estimation of how many vocalizing animals are being detected at any one time. While it may seldom be possible to discriminate the position of a mother from that of her calf, but dual click trains from the same location do at least indicate two animals that are proximate to one and other. Vocalizations may reveal short segments of the path taken by a porpoise. Such segments may become especially useful for a porpoise that swims very near a tidal power installation. Being able to determine the number of vocalizations detected within a certain volume of water is an important step towards estimating porpoise abundance. For tidal power applications, arrays of hydrophones allow an estimation of how harbour porpoise utilize the area near and around turbine installations. It would be very useful to measure how often harbour porpoise vocalizations come from very near the turbine versus further from the turbine. Thus, the hydrophone arrays provide a direct and convient way to measure the extent to which harbour porpoises demonstrate avoidance of, or ambivalence or attraction to, in-stream turbine installations.

4.4 Localization and abundance

To date, monitoring of harbour porpoises at the FORCE Test Site has been based upon measuring porpoise echolocation "activity". Ideally, one would want to be able to estimate porpoise abundance. That is to measure the number of porpoises within some defined area. Additionally, it is useful to measure porpoise depths in order to determine the extent to which they are likely to encounter a tidal turbine.

Measuring abundance requires measurement of how many porpoises are within a defined area. If we define the area as being cylindrical then it would be enough to measure the range and depth of every porpoise within that area. Assuming this could be done, then rigorous calculations for porpoise-turbine encounter probability becomes possible. Indeed, by comparing areas close to the turbine with those further away it becomes possible to measure the extent to which porpoises may or may not avoid an in-stream tidal turbine.

Unfortunately, the beamwidth of a click is only 16^{o} for a harbour porpoise [19] so it is quite possible that a porpoise can be within some area containing a hydrophone array and yet not be detected. Nevertheless, one might expect that the porpoise might have some estimatable probability of being detected when it is within the area. Presently we are not at a stage where such proportions can be reliably quantified. But a beginning can be made by finding ways to obtain position information from those clicks that are detected.

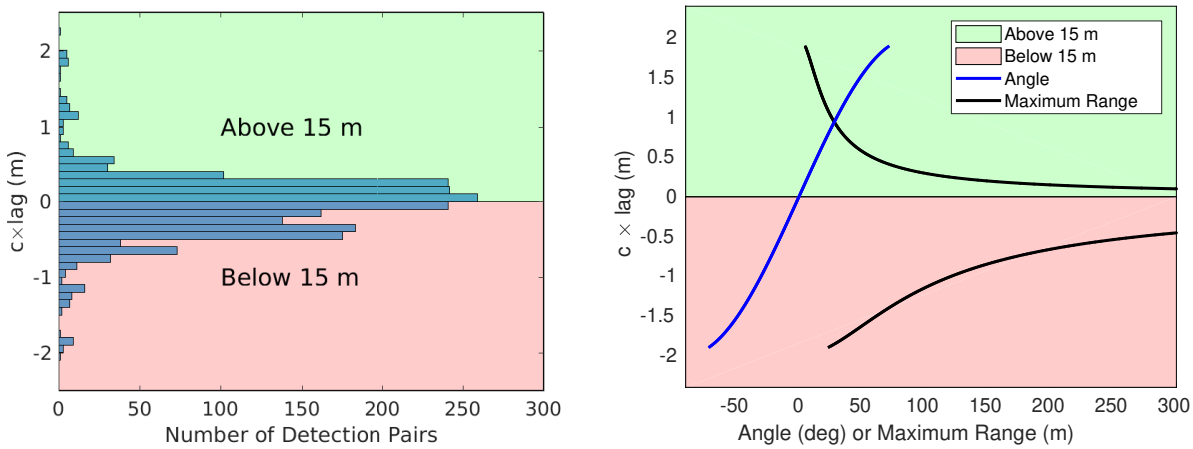

Figure 9: Left: Histogram of detections above and below the mid-level (15 m) of the two hydrophones. Right: Angle from hydrophone to porpoise (blue) and maximum range to porpoise (black).

4.4.1 Porpoise use of the water column

Our experimental drifter has two hydrophones that are separated by 2 m in the vertical. The mid-level of the two hydrophones was 15 m. If a harbour porpoise click arrives at both hydrophones and is from a porpoise that was below the mid-level (15 m), then it will arrive at the lower hydrophone first. Conversely, a click from a porpoise above the mid-level will arrive at the upper hydrophone first. Here we are assuming that detected clicks all took a direct path from porpoise to hydrophone but this may not always be the case.

Subsequent to the present analysis, we found that clicks can be reflected from the sea surface and seafloor (see §4.4.3 and [40]). Reflections from the seafloor are greatly scattered [40] and will not influence the present analysis. Reflections from the sea surface can sometimes be difficult to distinguish from signals that take a direct path from the porpoise to the hydrophone. Reflections from the sea surface will bias the present results towards porpoises being above the mid-level. A painstakingly detailed analysis would presently be required to rigorously evaluate which signals are direct and which are reflected from the sea surface. We are presently developing efficient, semi-automated methods to do that work for future studies.

The present work assumes that all click detections are for signals that take a direct path from porpoise to the two synchronized hydrophones. Our method was to consider each click received by one hydrophone and see if a corresponding signal was detected by the other hydrophone. For the purposes of evaluating correspondence, it is convenient to convert time lag τ_{lag} into a spatial lag $c\tau_{\text{lag}}$ by multiplying by the speed of sound c [24]. If the magnitude of the spatial lag is greater than 2 m then we discard those two signals from our analysis on the basis that they cannot be the same porpoise click travelling a direct path. This will eliminate many signals that take reflected paths (see §4.4.3 and [40]) but may not eliminate all of them.

The spatial lag $c\tau_{\text{lag}}$ indicates the angle θ_{path} of the path taken by and incoming click, with values near 0 being horizontal and values near -2 being from vertically below, for example.

$$\theta_{\text{path}} = \sin^{-1}\left(\frac{c\tau_{\text{lag}}}{2}\right) \tag{2}$$

The actual porpoise depth and range to the porpoise cannot be known but maximum range can be estimated because we know that a porpoise must be at most 15 m above mid-level of the hydrophones and the distance below is constrained by the seafloor.

Figure 9 shows a histogram for the number of clicks received as a function of spatial lag. About half the detections are of clicks that originate from more that 15 m below the air-water interface.

The plot on the right of Figure 9 shows the path angle (blue) as a function of spatial lag. Maximum range to the porpoise is calculated from path angle. For clicks arriving from above (positive spatial lag) the calculation of path angle is unambiguous. For clicks coming from below, we have assumed that the seafloor is 70 m below the mid-level of the hydrophones. This assumption could be avoided by obtaining depth of the water column at the position of the drifter when pairs of clicks were received. Indeed, the analysis could be extended to obtain a histogram of maximum range. Until questions about reflected signals are resolved, it is probably more prudent to not stray beyond this illustrative calculation. Nevertheless, these illustrative calculations explain the asymmetry of the histogram above and below the mid-level.

4.4.2 Detection pairs

Porpoises transmit their clicks as a narrow beam. Signal level falls by 3 dB within $\pm 8^{o}$ of the centre of the beam. Measurements made using a captive animal obtained a 16^{o} beamwidth in both the horizontal and vertical planes [19]. This would seem to present some intrinsic difficulties for using porpoise vocalizations to obtain position and abundance of animals.

A 16^{o} beam spans only 0.4% of the solid angle surrounding a porpoise. On the other hand, there is clear evidence that porpoise scan with their beam [31] so that within a short period of time the beam will sweep through a significantly larger solid angle. This will improve the likelihood that a porpoise is detected by a hydrophone but it also indicates that detections will become intermittent. From the receiver's frame of reference, this intermittency is expressed in terms of click trains.

The narrow beamwidth would seem to place limits upon the ability of separated hydrophones to both detect the same click in a reliable way. Other confounding factors might be: imperfect hydrophone performance, imperfect click detection algorithms, ambient sounds, signal distortion by propagation through variable currents or temperature/salinity gradients, and interference with other clicks or reflected clicks. We have, therefore, directly measured the probability that two separated hydrophones (and the Coda software) will detect the same click.

Presently we have detections from two hydrophones that are separated by 2 m in the vertical. A 16^{o} beam subtends 2 m at a range of 7 m. If beamwidth was the only limiting factor, the expectations should be that if a porpoise is much more than 7 m away then either both receivers would detect the click or neither of them would.

Table 7 is constructed by considering each hydrophone, in turn, as the primary instrument. The number of detections are separated according to signal level. At levels $\geq$ 125 dB both hydrophones obtain effectively the same number of detections (1204 vs 1188). Such strong signals suggest that the primary hydrophone must have been well within the beam and so the probability should be high that the other hydrophone might be also. Indeed, the probability that such strong signals are detected by both hydrophones is 0.82 ± 0.01 and is independent

Primary Hydrophone	Level	No. Detections	Prob. paired detection
icListenHF 1211	≥ 125 dB	1204	0.821 ± 0.011
icListenHF 1211	110-125 dB	1055	0.638 ± 0.015
icListenHF 1211	> 110 dB	2262	0.736 ± 0.009
icListenHF 1239	≥ 125 dB	1188	0.824 ± 0.011
icListenHF 1239	110-125 dB	1415	0.567 ± 0.013
icListenHF 1239	> 110 dB	2610	0.684 ± 0.009

Table 7: Probability that a porpoise click will be detected by a pair of hydrophones that are separated by 2 m. The probability is calculated as the probability that clicks detected by the primary hydrophone will also be detected by the second hydrophone.

of which hydrophone is designated as the primary instrument.

Hydrophone 1239 obtains substantially fewer detections than hydrophone 1211 when signal level is lower than 125 dB. Note, we set a cutoff level of 110 dB so weaker signals were rejected from our analysis. This difference is enough to suggest that hydrophone 1211 may not have been performing quite so well as 1239. It is also apparent that the probability of paired detection dropped to about 0.6 when signal level was 110-125 dB. Over all detections (levels > 110 dB) the probability of paired detection was about 0.7 (70%).

The minimum number of hydrophones required to obtain depth and range to a porpoise would be a vertical array of 3. If those hydrophones were spaced at intervals of 2 m, then the probability of all three receiving a click is the square of the probability that a neighbouring pair would receive the click. Thus, a pair probability of 0.70 becomes a triplet probability of 0.49. This reduction of probabilities over larger arrays illustrates the advantage to be gained by improving detection algorithms because an ideal detection algorithm should give a probability for dual detection that is greater than 0.7 for porpoises at all ranges larger than 24 m.

Results in Table 7 indicate that differences in instrument performance causes an asymmetry in the probability of paired detection when signal level is low — but not when the signal is strong. The fall off in detection probability for weaker signals can be, at least in part, attributed to setting a hard lower limit of 110 dB for a signal to be classified as "detected". When locating animals by using an array of many hydrophones, it may be advantageous to set the lower limit according to the strongest level recorded for each click over all hydrophones (and perhaps over all clicks within a click train).

It should also be observed that the Coda click detection software was designed within the constraints of the on-board computational resources of an icListenHF hydrophone. We are presently working on a more elaborate click detection algorithm which requires an order of magnitude more computational effort, uses more robust statistical and mathematical methods, and has every prospect of being more reliable.

4.4.3 Reflected clicks to calculate range and depth

We achieved a few estimations of both porpoise depth and range that are beyond the project's deliverables. While reviewing clicks detected by Coda for his Honours thesis [24], co-author Mike Adams made two odd discoveries:

1. Signals that looked like a porpoise click on a spectrogram but were smeared out when closely examined in the time domain.

2. Click trains that appeared to be closely spaced doublets separated by a much longer inter-click interval.

Both phenomena remained riddles that were not resolved until recently. We document the matter in the present report as well as in a recent journal publication [26].

The top panel of Figure 10 shows vertical lines in the spectrogram that are quite typical for a porpoise click but also shows signals that appear in the frequency band of porpoise clicks but are smeared out over a time interval far greater than the typical 100 μs duration of a porpoise click. It is also apparent that after a regular interval the typical clicks are sometimes followed by a smeared out signal. In many other spectrograms, only the smeared out signal was seen.

To obtain another view of these signals, we filtered the time series to keep frequencies within and near the propoise frequency band. A Hilbert transform was then used to construct the signal envelope. The middle panel of Figure 10 shows the envelope for the first click and the following smeared signal as measured by the upper hydrophone (blue) and lower hydrophone (red). The envelope from the lower hydrophone is plotted upside down for the sake of clarity.

The most likely explanation for these signals seemed to be that the first pulse-like signal was a porpoise click that had followed a direct path to the hydrophone whereas the smeared out signal was the same click that had reflected (scattered) off the seafloor. The geometry is illustrated by the lower panel in Figure 10. Considering the narrow beamwidth of harbour porpoise clicks [19], it seems most unlikely that the same click could reach the hydrophones by both direct and reflected paths unless the porpoise was near the sea surface (above the hydrophones) and directing its click on a downwards slant. Such a geometric configuration would seem most likely when a porpoise was beginning its dive from the sea surface.

Even though reflections from the seafloor were smeared, it was sometimes possible to identify an apparently clear time of arrival. Given two times of arrival along direct paths, and two times of arrival along reflected paths, the geometry shown in the lower panel of Figure Figure 10 illustrates how a vertical array of two synchronized hydrophones may be used to calculate: the time t_0 when the porpoise clicked, and the depth z and range R of the porpoise from the hydrophones. The mathematics for reflections from the seafloor are documented in our recent publication [26].

Signals that had been previously interpreted at double-clicks within the click train [24] were subjected to a similar analysis. Again, signals from both hydrophones were filtered to preserve frequencies within the porpoise band and envelopes were calculated using the Hilbert transform. The top panel in Figure 11 shows the envelope functions from the two hydrophones, with the envelope for the lower hydrophone (red) tipped upside down for visual clarity. The result is a train of doublet clicks. Zooming in on the first doublet (middle panel) we see small but clear differences in the times of arrival at the upper (blue) and lower (red) hydrophones. Times of arrival seem consistent with the first peak of the doublet being a click that follows a direct path and the second peak being a reflection from the sea surface (bottom panel of Figure 11). The narrow nature of a porpoise beam [19] would seem to require that the porpoise be below the hydrophones in order for the same click to arrive by both a direct path and a reflection from the sea surface.

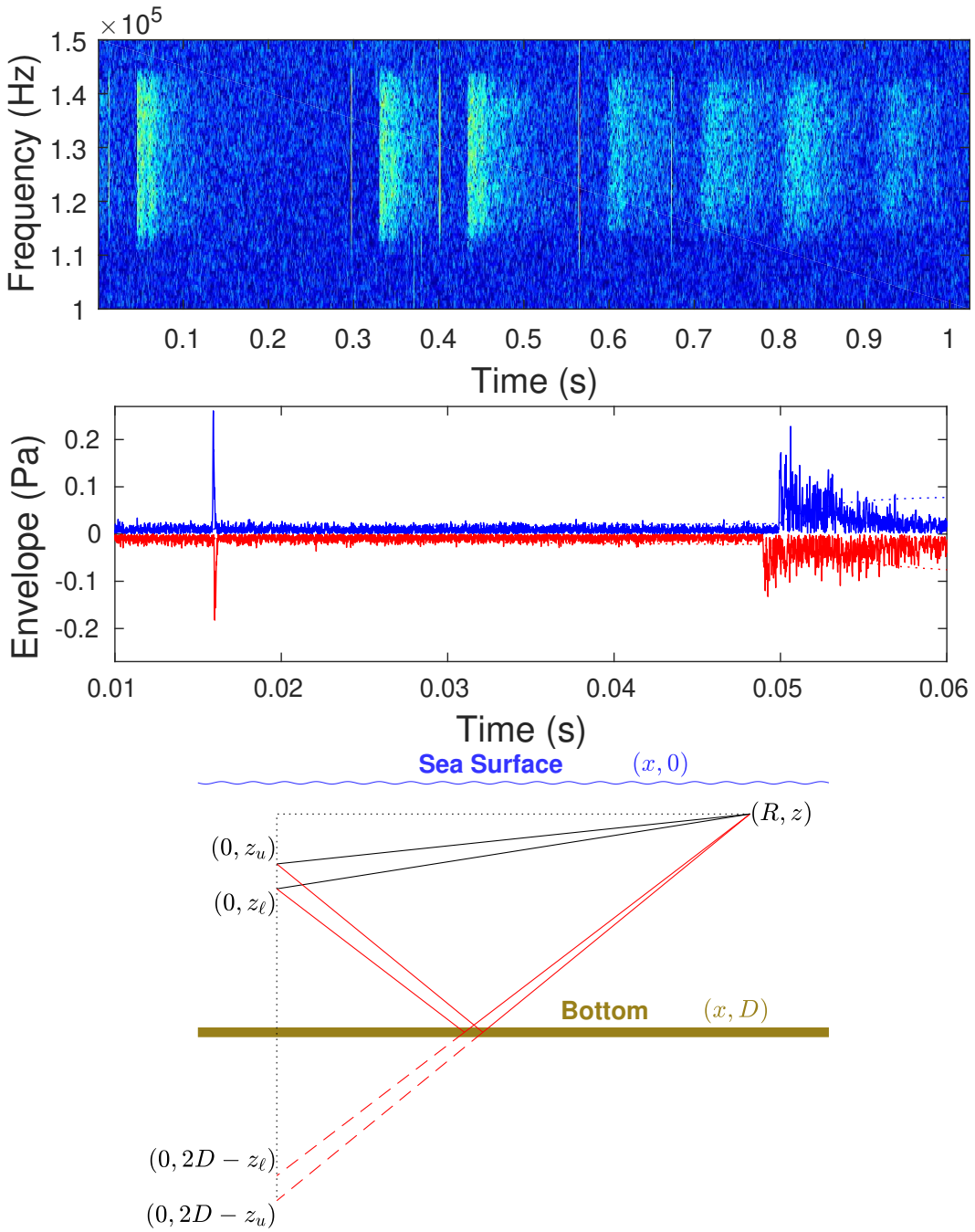

Figure 10: Top: Spectrogram showing porpoise clicks which appear as vertical lines and signals of much longer duration. Middle: Zooming in on the envelope for the first click in the time series. Bottom: Direct signal paths (black) and paths for signals reflected from the seafloor (red).

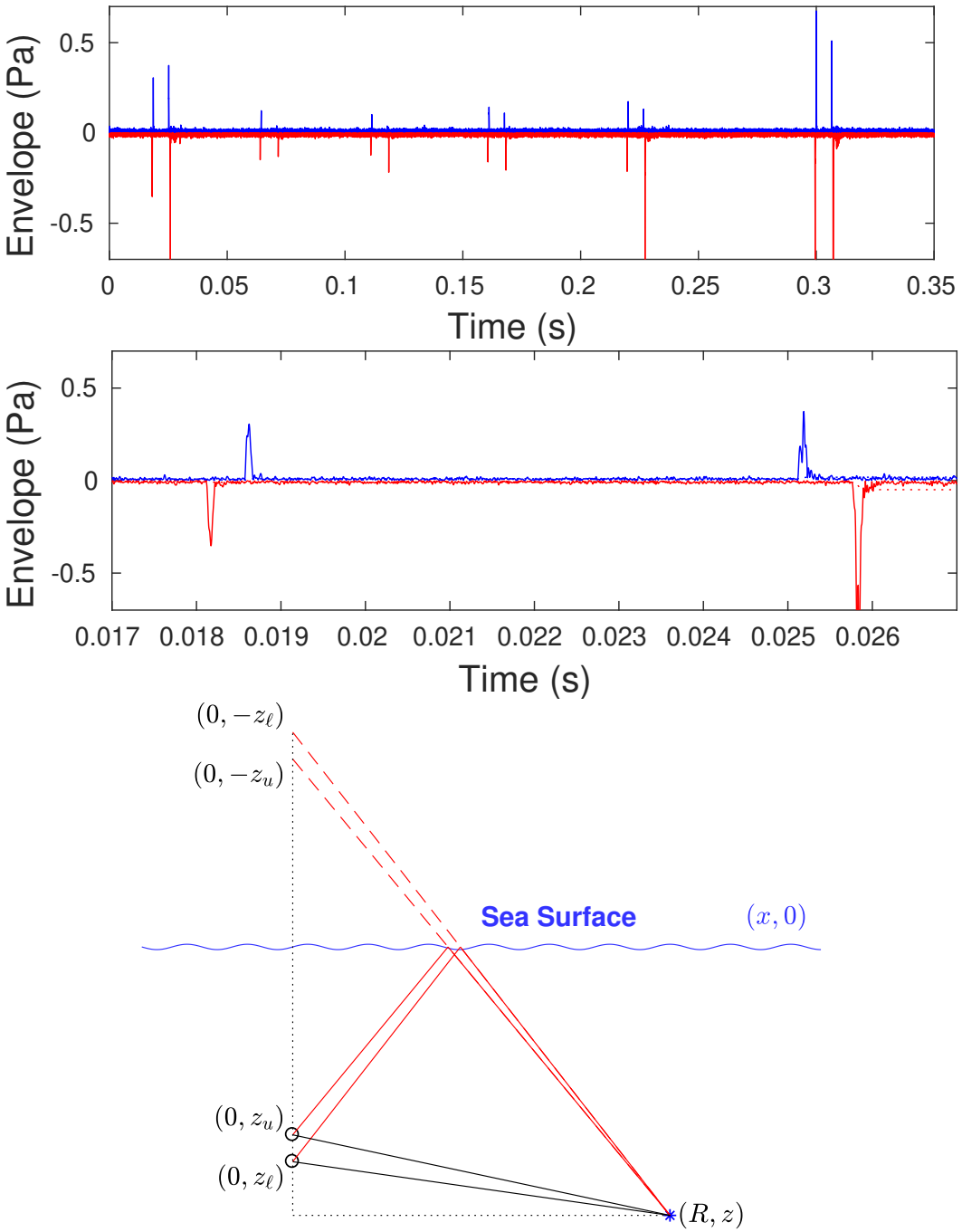

Figure 11: Envelope of porpoise-band filtered time series measured by upper (blue) and lower (red) hydrophones. For ready visualization, the red line plots the envelope upside down. Top: Envelopes show a train of paired peaks. Middle: Zooming in on the envelopes for the first pair in the click train. Bottom: direct signal paths (black) and paths for signals reflected from the sea surface (red).

Signal envelopes of the reflections from the sea surface seem to have suffered little distortion (Figure 11). It follows that there may be many instances when accurate times of arrival can be determined for both the direct path and for reflections from the sea surface. With such times of arrival at a vertical array of two hydrophones it is possible to calculate the time t_0 at which the click was transmitted as well as the depth of the porpoise and range from the hydrophones. The appropriate equations have been published elsewhere [26] and are be presented here in view of their likely frequent utility.

The following pythagorean equations apply to direct paths from a porpoise at depth z and horizontal range R from the hydrophones

$$(z - z_u)^2 + R^2 = c^2(t_u - t_0)^2 \quad (3)$$
$$(z - z_\ell)^2 + R^2 = c^2(t_\ell - t_0)^2 \quad (4)$$

Here, the depths of the upper and lower hydrophones are z_u and z_ℓ and corresponding times of signal arrival are t_u and t_ℓ. Similarly, the equations for signals reflected from the air-water surface are

$$(z + z_u)^2 + R^2 = c^2(t_{ru} - t_0)^2 \quad (5)$$
$$(z + z_\ell)^2 + R^2 = c^2(t_{r\ell} - t_0)^2 \quad (6)$$

were t_{ru} and $t_{r\ell}$ are times of arrival for a signal that is reflected from the sea surface. Thus we have four equations with which to solve for the three unknown variables (R, z, t_0). Expanding and rearranging we can write the above equations in matrix form

$$\begin{pmatrix} -2z_u & 2t_u c^2 & 1 \\ -2z_\ell & 2t_\ell c^2 & 1 \\ 2z_u & 2t_{ru} c^2 & 1 \\ 2z_\ell & 2t_{r\ell} c^2 & 1 \end{pmatrix} \begin{pmatrix} z \\ t_0 \\ C \end{pmatrix} = \begin{pmatrix} -z_u^2 + c^2 t_u^2 \\ -z_\ell^2 + c^2 t_\ell^2 \\ -z_u^2 + c^2 t_{ru}^2 \\ -z_\ell^2 + c^2 t_{r\ell}^2 \end{pmatrix} \quad (7)$$

where

$$C = z^2 + R^2 - c^2 t_0^2 \quad (8)$$

This overdetermined system of equations is a linear regression and can be solved using singular value decomposition [29] to obtain (z, t_0, C) and thus R.

It is also notable that our experimental configuration had hydrophones separated by only 2 m in the vertical. Thus, the angle subtended by the two direct rays (bottom panels in Figures 10 and 11) is very small, corresponding to a small aperture. The reflected rays, on the other hand, can be considered to correspond to a virtual pair of hydrophones well above the sea surface (or well below the seafloor). Thus, by considering reflected rays the hydrophone array acquires much larger aperture.

Using the direct paths and a reflected path enables the depth and range of a porpoise to be estimated. Hydrophone measurements also give signal level of each click. Figure 12 compares signal level of each click with range. The level at the centre of a click beam was also estimated as a function of range by assuming maximum source level 178-205 dB [28], radial beam-spreading, and absorption of 37.5 dB/km [41]. Comparing signal level with range (Figure 12), we found that the source level of porpoises in Minas Passage/Channel is generally consistent with maximum source level in the range 178-205 dB, as measured in Dannish waters [28].

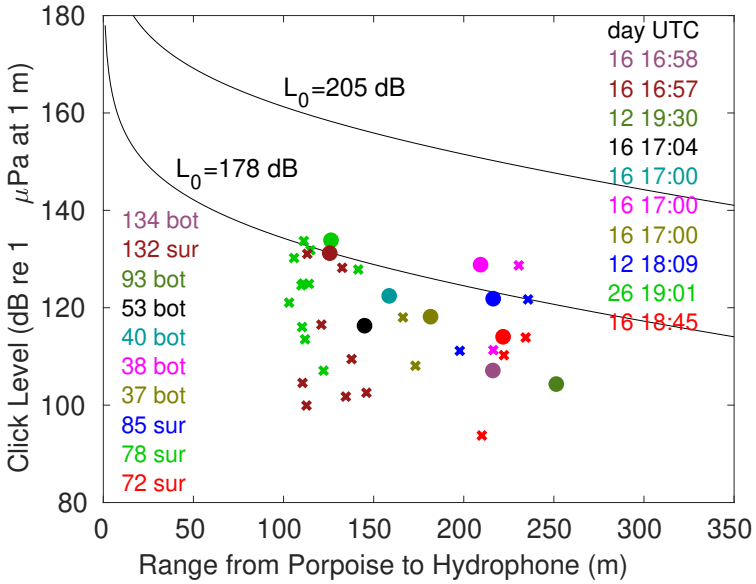

Figure 12: Click level as a function of range. Crosses show results for individual clicks. Filled circles show maximum level and averaged range for each click train. The black lines shows theoretical maximum signal level based upon source levels of 178 dB and 205 dB.

A porpoise typically cruises with speed ≤ 1 m/s [20]. Given that a train of clicks typically arrives within less than one second, we might consider each click to give an independent estimate of the same depth z and range R to a porpoise. The measurements which we presently analyse consist of 10 click trains with N clicks available in each train for obtaining z and R. For our present results, N is in the range 1 to 10 useful clicks per train. Table 8 documents the average values of z and R for each click train, along with standard deviations. Relatively few of the reflections from the seafloor had clearly definable arrival times so most of those trains contained only a single useful click. Nevertheless, results allow some useful interpretation.

Reflections from the sea surface were always from a porpoise that was below the level of the hydrophones whereas reflections detected from the seafloor were from porpoise located near the sea surface. This indicates animal orientation in the vertical. Thus, it also supports the notion that Figure 9 might contain some bias. Clicks from the sea surface are sometimes so clean that context is required to differentiate them from clicks taking a direct path whereas reflections from the sea floor were always messy signals. Thus, Figure 9 probably over represents the number of detections above the 15 m level.

It should also be noted that at least a portion of the porpoise clicks detected by the C-PODs (and Coda-icListenHFs) would have been reflected signals. Porpoise click detection is often considered to be a measure of porpoise "activity". At best it is only proportional to a qualitative metric, so the fact that C-POD measures fewer DPM than Coda-icListenHF is not in itself of particularly great importance. The real advantage comes when clicks can be used to calculate porpoise positions.

In section §5 we will briefly describe our recent measurements in Minas Passage using a vertical array of 4 hydrophones that are spaced at 2 m intervals spanning a 6 m aperture. The present project scope does not extend to the analysis of those measurements but it

Ref. #	R (SD)	z (SD)	N	Reflected from
72	222 (12)	23 (1.3)	3	Sea surface
78	127 (24)	33 (6.4)	3	Sea surface
85	216 (27)	21 (2.6)	10	Sea Surface
132	126 (13)	48 (5.1)	8	Sea Surface
37	182 (21)	8 (8)	3	Seafloor
38	210 (25)	-1 (10)	3	Seafloor
40	159 (—)	14 (—)	1	Seafloor
53	145 (—)	6 (—)	1	Seafloor
93	252 (—)	3 (—)	1	Seafloor
134	217 (—)	2 (—)	1	Seafloor

Table 8: Range R and depth z of porpoises as determined from click trains. $N > 1$ sea surface or seafloor reflections were available for 6 of the trains but 4 trains only had one well-resolved reflection from the seafloor. The number of clicks with reflections is given by N. Standard deviations (SD) are indicated. Ref. # is associated with observation time and enables this table to be associated with points plotted in Figure 12.

is appropriate to diagnose the performance of such an array. We have formulated general equations for a vertical array consisting of any number of hydrophones. With 4 hydrophones spaced 2 m apart we can directly calculate travel times from a given porpoise location (R, z) to each hydrophone. Then, we can add error to these travel times and compute estimates of the porpoise location which includes a difference from the true range. This difference is the error in range calculation that is caused by the specified error in time of arrival. Undertaking many such calculations enables a statistical evaluation of how timing errors are translated to position errors. This method is commonly called a Monte Carlo simulation.

Presently let us consider random errors in time of arrival that have typical magnitude 5 μs (corresponding to about 1 cm of error in hydrophone alignment relative to the vertical). The left panel of Figure 13 shows error growing rapidly for ranges greater than 80 m. Ostensibly, the green zone represents a band of ranges that the array might calculate with useful accuracy. At ranges less than 20 m we leave a blank area in view of the *possibility* that a narrow porpoise beam may not span more than 3 of the hydrophones and the wiggle in the error bars at ranges less than 30 m corresponds to a *possibility* that the narrow beam may only be detected by 3 of the four hydrophones. Future analysis[4] of the experimental measurements described in section §5 may enable these *possibilities* to be evaluated as either being matters of no concern or issues that will probably require an array of more than 4 hydrophones in order to be resolved.

Limitations on the useful range may appear to be set in a conservative way in the left panel of Figure 13. Indeed, at 80 m range the typical error is less than 20%. The reason for conservatism becomes more obvious by looking at the error for ranges larger than about 140 m. At such ranges the lower limit on probably range (lower dashed line) takes a downward turn. The turn steepens with increasing range so that beyond 160 m there becomes an increasing likelihood that a signal from 160 m away might appear to be only 80 m away.

Extending the array to 6 hydrophones (aperture 10 m) extends performance at larger ranges but ultimately leaves us with a similar problem. Extending the aperture by moving

[4]Such analysis is beyond the scope of the present project.

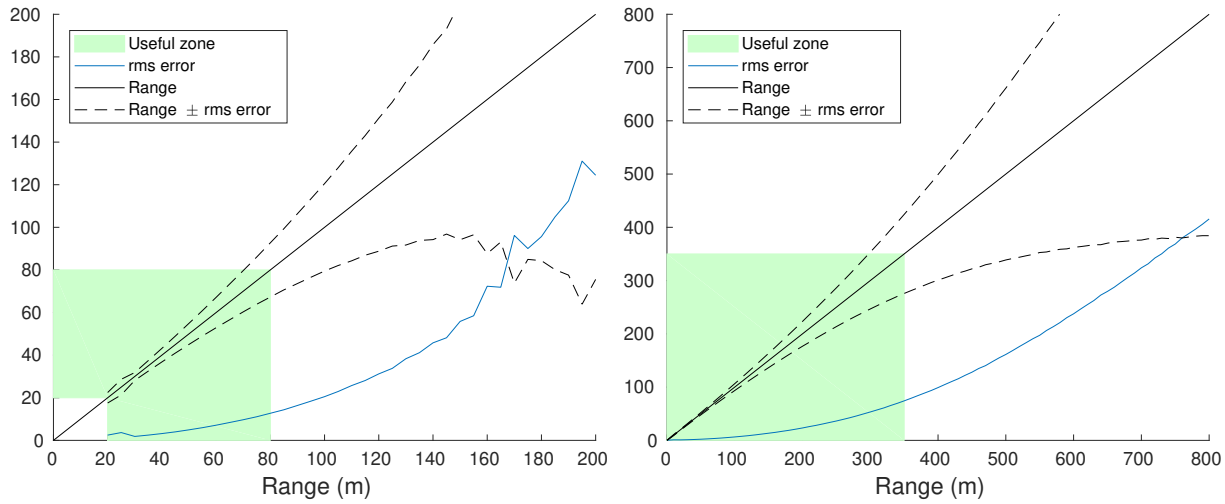

Figure 13: Root mean square error in porpoise range (blue). The black line shows range against range with the dashed lines showing range plus and minus the rms error. The Monte Carlo simulation assumed time of travel had uncertainty 5×10^{-6} s for signals taking a direct path to the hydrophones. Depth of the porpoise was set to 15 m below the top hydrophone and the top hydrophone was set at 15 m below the sea surface. LEFT: Range was simulated from a vertical array of 4 hydrophones spanning 6 m. RIGHT: Range was simulated using the same vertical array of 4 hydrophones plus a virtual array obtained from surface reflections. Reflected signal had time of arrival uncertainty increased to 5×10^{-5} s.

the upper and lower hydrophones further from the middle hydrophones might also help.

Using the times of arrival of clicks reflected from the sea surface will greatly increase aperture. In this way, a four-hydrophone array is effectively turned into an eight-hydrophone array. The top part of the array is above the sea surface so we should call that part a *virtual array*. Providing times of arrival can be calculated to within a reasonable accuracy, reflected signals may greatly increase the effectiveness of hydrophone arrays for measuring porpoise position. The right panel of Figure 13 illustrates how reflected signals might enhance the performance of the same four-hydrophone array that is plotted in the left panel. Note, the calculation for the right panel assumed that the reflected paths had time of arrival errors 10× larger than those for the direct paths. Measurements made in §5 are expected to be useful for future testing of these ideas.

If subsequent work confirms the basic idea simulated in the right panel of Figure 13 then a very clear path is indicated towards quantifying porpoise abundance. Rigorous calculation of abundance would still require a few additional steps because the narrow beamwidth of porpoise vocalizations makes their detection a statistical game so we require additional information about how porpoises orient themselves and with what timescales their orientation changes.

A complete measurement of abundance is not required in order to resolve the question as to the circumstances under which a porpoise may or may not avoid an in-stream tidal turbine installation. For that work, only a relative abundance is required. That is to say, a determination of the relative likelihood that click trains come from ranges near and far from the installation. That metric seems tractable to us.

Our observations of reflected porpoise clicks show signals reflecting either off the seafloor

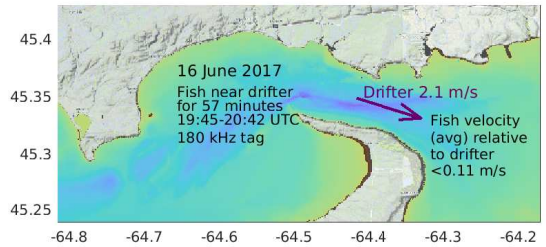

Figure 14: Drifter displacement (arrow) during the 57 minutes when a tagged fish was detected by an icListenHF that was suspended below a drifter.

or off the sea surface, but not both for the same click. Sperm whales have been observed to emit clicks so that the one click takes a direct path and reflects off both the sea surface and seafloor [42]. This testifies to the sperm whale emitting a good deal of sound that travels off the axis of the main beam. We expect that our new measurements (§5) will enable estimation of the off-axis signal level for harbour porpoise vocalizations.

It should be noted that our position finding work above has used a "direct method". Direct methods use times that a signal is received by each hydrophone in an array in order to calculate the source location and time at which a signal was emitted. Macaulay et al., [43] claim that the direct method (1) can't deal with ambiguous results, (2) has complex propagating errors, and (3) requires different equations for different arrays. Instead of the direct method, Macaulay et al., [43] promote the "forward" method which iteratively searches for the source location that matches measured time delays to delays that have been pre-computed for all possible source positions. We observe the "forward" method is very demanding on computational resources. Contrary to the first claim by [43], our work has shown that direct methods can deal with the evaluation of ambiguities caused by measurement error. We totally agree that measurement uncertainty can cause complex propagating errors but would hasten to add that such errors can be efficiently explored using the direct method. Sanderson has coded fast algorithms that use the direct method [44] and explore the effects of measurement error (Figure 13). As for their third point, different equations are required for different arrays, regardless of whether the method is 'direct' or 'forward'.

4.4.4 Drifting hydrophone detection of tagged fish

We observed an 180 kHz signal in our 16 June 2017 hydrophone measurements that looked like a sequence of PPM pulses from a Vemco fish tag. A matched-filter edge-detector was constructed so that we could measure intervals between pulses. Dale Webber (Vemco Ltd) confirmed that the signal was from a salmon smolt that had been tagged by the Department of Fisheries and Oceans.

The tag was detected repeatedly over a 57 minute period when the drifter was in Minas Passage during the latter part of the flood tide (Figure 14). Consideration of the interval over which detections were obtained, along with signal strengths, enabled application of two rough methods for estimating the average fish velocity relative to the drifter [45]. One method indicated average velocity within the range 0.025 to 0.11 m/s. The other method obtained average swimming velocity of 0.051 m/s with 95% confidence interval $[0.034, 0.067]$ m/s.

A brief report [45] was prepared for as a contribution towards DFO studies of salmon smolt and their migration from river to open ocean. DFO confirmed that the tag was implanted into a 16.2 cm smolt at the Stewiacke River on 23 May. The smolt reached the Stewiacke-Shubenacadie confluence on 25 May and was detected at the mouth of Shubenacadie River

icListenHF Ser. No.	Depth (m)	Owner
SBW 1211	12	Acadia University
SBW 1239	13.50	Acadia University
SBW 1307	15.40	OceanSonics
RBW 1492	17.32	OceanSonics

Table 9: Hydrophones used for the vertical array.

on 29 May. Thus approximate average travel speeds were:

- 0.058 m/s from the confluence of Stewiack and Shubenacadie Rivers to the mouth of the Shubenacadie.
- 0.043 m/s from the mouth of the Shubenacadie to Minas Passage.

These average travel speeds are broadly similar to our estimates of swiming speed relative to the drifter.

There are several types of Vemco fish tags. The 69 kHz tags use a Pulse Period Modulation (PPM) encoding. PPM signals typically consist of a sequence of pulses (duration about 4-5 milliseconds) and the interval between pulses encodes information which Vemco can decode. The High Resolution (HR) tags use PPM encoding with a 180 kHz carrier wave and also transmit a 170 kHz pulse that has duration of about 5 milliseconds with many embedded phase shifts that encode information. It is relatively straighforward to search icListenHF hydrophone recordings for PPM signals from acoustic fish tags. It may be advantageous for fish researchers if hydrophone detections could be submitted and processed as a part of the data management operations of the Ocean Tracking Network.

5 Drifter Field Test with 4 Synchronized Hydrophones

A vertical array of four synchronized hydrophones was deployed on a drifter. Measurements were made on three days, one more than originally proposed.

5.1 Drifter design and construction

A pole-float drifter with subsurface buoyancy and hydrophone ladder was designed and constructed for these experiments (Figure 15). The pole-float was made from 1×4 inch spruce backing pole with high density construction styrofoam for additional flotation. The pole float was painted high-visibility orange and its top part had accommodations for attaching a GPS logger and a real-time Tractive tracking system.

Three 20 cm diameter trawl floats provided additional subsurface buoyancy as illustrated in the top left panel of Figure 15. Plastic hydrophone clamps were borrowed from OceanSonics Ltd and used to construct a hydrophone ladder that suspended hydrophones at levels indicated in Table 9. All hydrophones had been recently calibrated before deployment. Two icListenHF hydrophones were also borrowed from OceanSonics, along with a Smart Cable that is used to synchronize the hydrophones. A lead weight was tied at the bottom of the hydrophone ladder.

The Tractive tracking system was attached to the top of the pole float so that we could use a smart phone app to obtain the drifter position at any time. A line with additional surface

flotation was attached to the pole float (top right panel of Figure 15) in order to provide emergency backup buoyancy should one of the subsurface floats flood.

The subsurface floats and lead weight serve to hold the hydrophones as a vertically aligned array. Note, the drifter has no drag unit. This minimizes any tendency for current shear to disrupt the vertical alignment. A HOBO Pendant G-Logger served as a tilt sensor. The tilt sensor and a GoPro (Hero3 White Edition) video camera were mounted onto a length of wood which was fastened to the vertical line that extended downwards from the subsurface flotation (bottom middle panel of Figure 15). Plastic guides fixed near the ends of the wood made alignment more accurate. The tilt sensor measures any disruption of the hydrophone array that might be caused by swirling eddies. The GoPro camera was oriented downwards to provide visual confirmation that there was no disruption of the hydrophone array (due to drifting material, for example). There was also a possibility that camera footage might show marine animals.

The second function of the subsurface floats is to enable a larger bottom weight in order to increase the inertial mass of the drifter system. This is an important design feature because it minimizes vertical jiggling of the hydrophones by wind waves. In our study area, the water is deep so wind waves will satisfy the long-wave dispersion relationship [46]

$$\omega^2 = gk \tag{9}$$

that shows wavenumber k is nonlinear function of angular frequency ω. Phase speed of the wave is $c = \omega/k$ so we can obtain $\omega = g/c$. Thus, faster waves have lower frequency. It seems obvious that the wind cannot put energy into waves unless the wind speed U is greater than c. Thus we expect that the wave period T will be constrained to $T \leq \frac{2\pi U}{g}$. The relationship does not take into account dissipation and energy transfer between waves of different frequencies and so an empirical fit to observations is required. Neumann and Pierson [47] give

$$T = 0.81\frac{2\pi U}{g} \tag{10}$$

A full treatment of drifter motion can be rather sophisticated, especially when there are multiple elements with weak coupling between them [48]. Simplifying to consider the vertical displacement h of the pole-float drifter without friction but with forcing by a wind-wave of amplitude a and angular frequency ω gives

$$\frac{d^2h}{dt^2} = -\Omega^2 h + a\Omega^2 \cos(\omega t) \tag{11}$$

$$\Omega^2 = \frac{g\rho A_{\text{pole}}}{M} \tag{12}$$

where Ω is the angular frequency with which the pole float oscillates, A_{pole} is cross-sectional area of the pole float, inertial mass M of the entire drifter, and ρ is seawater density. Substituting a solution of the form $h = \alpha\cos(\omega t)$ gives

$$\alpha = \frac{\Omega^2}{\Omega^2 - \omega^2}a \tag{13}$$

Thus a surface wave with vertical amplitude a causes the pole float to oscillate vertically with amplitude α.

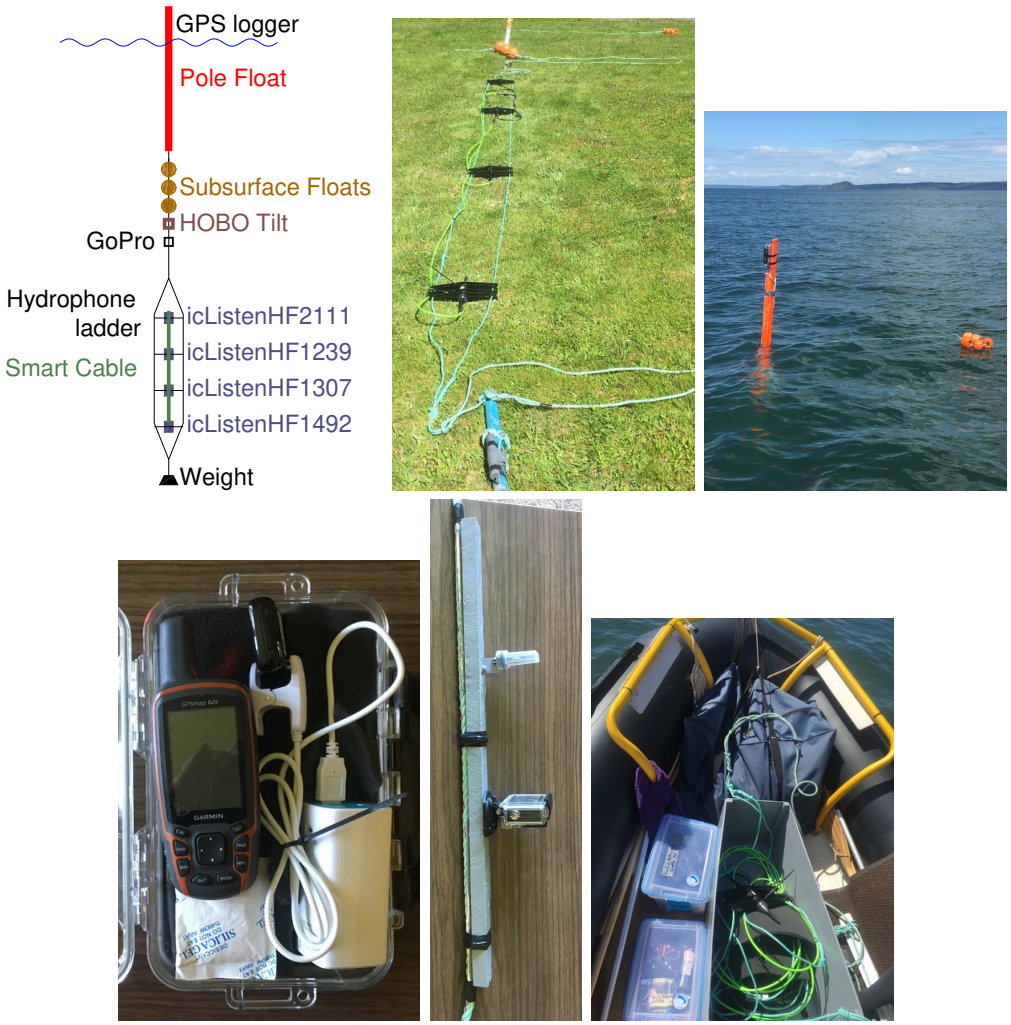

Figure 15: Pole-float drifter with vertical hydrophone array. TOP-LEFT: Schematic of drifter with hydrophones. TOP-MIDDLE: Photograph of drifter with hydrophones laid out on shore. TOP-RIGHT: Deployed, pole float holding Maximum box with GPS systems. The attached recovery line includes emergency flotation, sufficient should one subsurface float flood. BOTTOM-LEFT: Garmin GPS logger, Tractive GPS/Smart Phone 3G tracking system, and USB power pack inside a Maximum watertight box. BOTTOM-MIDDLE: HOBO Pendant G-Logger and GoPro video camera (Hero3 White Edition) mounted to the drifter line. BOTTOM-RIGHT: Equipment laid out in the bow of the RHIB, shortly before deployment.

Performance of the drifter will be better than indicated by the above idealized equations because a drifter also has frictional damping. Nevertheless, the nonfrictional relationships indicate a worst case performance, as follows. The cross-sectional area A_{pole} of the pole float was 0.0064 m^2 and the inertial mass M of the entire drifter layout was 20 kg. Substituting into (12) gives a 3.5 s buoyancy period. Calm weather was preferred for our drift experiments so the wave period obtained from (10) was much less than the buoyancy period $2\pi/\Omega$ obtained from (12). From equation (13) we see that the drifter displacement is a small fraction of that of the wind wave. Indeed, considering frictional effects further reduces oscillating drifter movement [48]. Hydrophones had little motion relative to the water in which they were immersed so it is expected that flow noise [17] was largely avoided.

5.2 Experimental method

The complete drifter system was assembled on land and tested. Our research vessel was a small Rigid Hull Inflatable Boat (RHIB). As it is difficult to handle such a large and complicated experimental apparatus from a RHIB, it was necessary to assemble some parts of the drifter-hydrophone system as it was deployed. The lower-right panel of Figure 15 shows some components as they are arranged in the RHIB prior to being deployed.

After deploying the drifter (in Minas Passage or Minas Channel), the RHIB engine was turned off. A custom-designed sea anchor was used to slow the wind-driven drift of the RHIB. A Garmin GPS logged boat position at 5 s intervals. The engine of the RHIB was only briefly operated to bring it back to the drifter when there was a danger of losing visual contact.

Visual observations of porpoise and observations of wind and sea state were made concurrent with the drifter measurements. Some Secchi depth measurements were also made. This is a high-value data set because it provides information about porpoise position relative to the drifter and, therefore, represents a first but significant step towards measuring the local porpoise abundance.

5.3 Measurements and preliminary analysis

The drifter was deployed during the flood tide on 6 and 7 June 2018 and on the ebb tide on 10 June 2018 (Figure 16). Analysis of these measurements is ongoing and is expected to be reported in future studies, including a M.Sc. thesis by Mike Adams (Acadia University). A brief, preliminary analysis is outlined below.

The drifter trajectories in Figure 16 are of some interest in their own right. The flood tide trajectories begin with a characteristic anticlockwise loop in Minas Channel. As they approach Cape Split, the trajectories align with the channel thalweg. Rapid acceleration at Cape Split results in inertial overshoot to the north of the thalweg at the western end of Minas Passage. This inertial effect is also the dynamical mechanism which results in the well-known nearshore eddy in the southwest edge of Minas Passage on the flood tide. Progressing into Minas Passage, the drifter track aligns with the main channel. Both of the presently measured flood tide trajectories pass along closely parallel tracks into Minas Basin. High tide is approaching by the time the drifters enter Minas Basin so we do not expect trajectories to be strongly constrained by jet-like vorticity dynamics. Later, we will see that similar long term drifter tracks tend to fan out as they enter Minas Basin on the tail end of the flood tide.

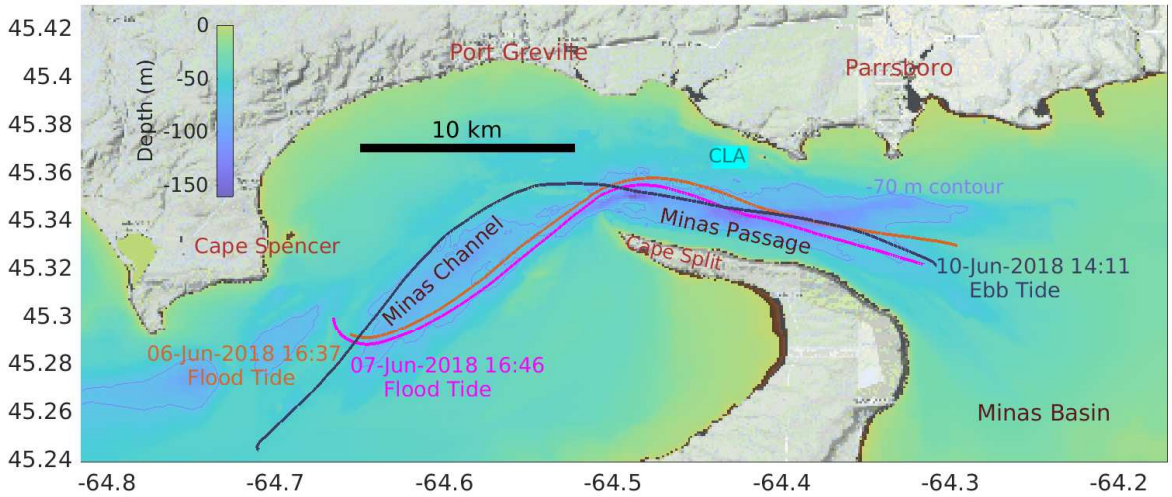

Figure 16: Tracks of the drifter which suspended a vertical array of 4 synchronized hydrophones. Tracks are colour coded with deployment date and time indicated at the beginning of each track.

It is dynamically relevant to drifter tracks that the bathymetry also fans out passing from Minas Passage to Minas Channel.

The ebb tide trajectory (Figure 16) passes from Minas Passage to Minas Channel when the tide is running strongly. This part of the ebb tide trajectory is a jet so inertia carries the drifter more directly westward and into more shallow waters. Tidal currents are largely barotropic, so the rising bottom strains current throughout the water column. Strong, large scale eddies are abundant at this location. The strong differential kinematics of that flow frequently caused our hydrophone array to tilt and our preliminary analysis shows high levels of associated ambient sound. While ambient sound and tilt are not convenient for our original objective, we expect that the association of tilt and increased ambient sound will make for a separate study that is useful and interesting for its own merits. Indeed, such natural events that increase ambient sound provide context critical for evaluating the ecological consequences of increased sound level attributed to tidal current turbines [49] and other anthropogenic sources [50, 51, 52].

Most of the time, the hydrophone array was very close to vertical. Figure 17 shows tilt measured during the 6 June 2018 flood tide drifter deployment. The top plot shows angle from the vertical as seen with a time scale that extends over 5 hours. At about 20:00 and 20:35 there are large departures from the vertical that preclude using the hydrophone array for obtaining range and depth of any porpoises that may be detected. These times are associated with the strongly turbulent current when the drifter passes near Cape Split and into Minas Passage. Nevertheless, much of the time any departure from vertical is at the level of instrument accuracy, a fraction of a degree. Even though the upper plot seems to show angles frequently near 2^o, this is not really so. Expanding the time scale (lower plot in Figure 17) shows that the departures to 2^o are infrequent compared to the more commonly near-vertical values.

Measurements of tilt indicate that most of the time our synchronized hydrophones might be useful for obtaining range to a porpoise and the depth of the porpoise. There is less drag on one large float than on three smaller floats with the same buoyancy. It follows that vertical

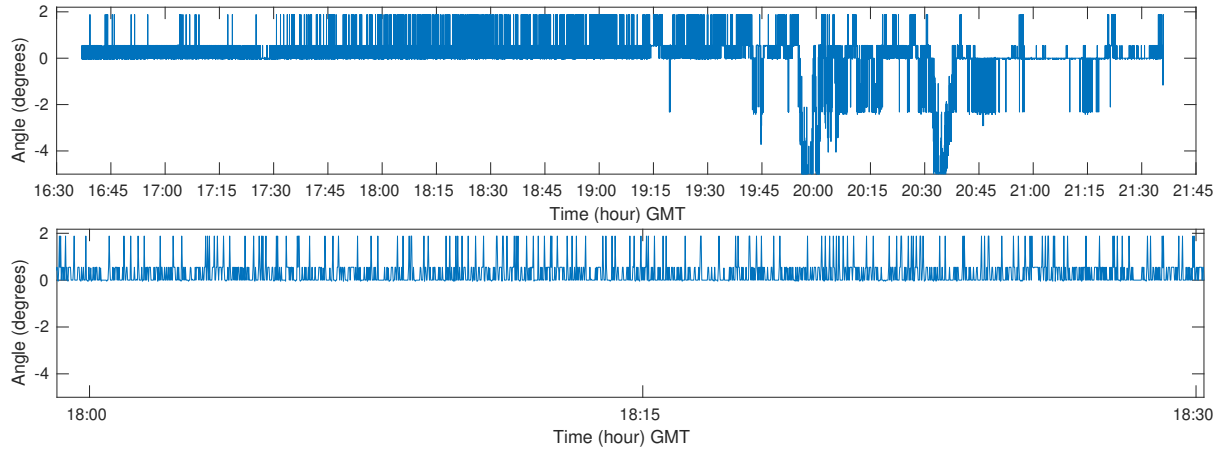

Figure 17: Tilt from vertical for the hydrophone array measurements on 6 June 2018. Upper plot shows the entire time series. The lower plot shows a portion of the time series at higher temporal resolution. Most of the time the departures from vertical are near the limit of measurement accuracy.

orientation would have been better had we used one large subsurface float instead of three smaller floats. On the other hand, multiple floats reduce the risk of equipment loss.

The Coda click detector was run over the 2018 hydrophone measurements and we found that the proportion of detection positive minutes (DPM) was comparable to the 2017 measurements.

The Coda click detector was designed within the constraints of having to operate in real time within an icListenHF hydrophone. To date, it has been largely applied without those constraints, being run on an external computer (with much more processing power than an icListenHF). Furthermore, it has been applied in a serial manner to multiple data streams. We have, therefore, used a modified application of the click detector to exploit more information by operating both on longer segments of measurements and assessing information obtained from multiple hydrophones at the same time. The entire data set has been processed in this way but we regard these results as just a stepping stone towards a much more rigorous mathematical method of porpoise detection, so they won't be reported in any detail here.

These concepts are presently applied at the click-review stage but, if advantages become clear, will be applied more upfront. Ultimately, we envision software that operates immediately following collection of measurements using the OceanSonics *Array Data Manager*.

Presently the click-review software uses measurements made by the vertical array of hydrophones, in order to obtain times at which a click detected by Coda arrives at each hydrophone in the array. Acadia/OceanSonics localization software is then used to calculate range from the drifter to the porpoise and the depth of the porpoise when it emitted the detected click (Figure 18). These are very preliminary calculations and a complete analysis must involve a great deal of careful error analysis before they can be safely interpreted. Furthermore, the above review software indicates that a good many usable clicks were missed by Coda. Improved algorithms are under development. It is expected that more comprehensive and statistically tighter results will ultimately be achieved and reported in Mike Adams' M.Sc. thesis (anticipated spring 2020).

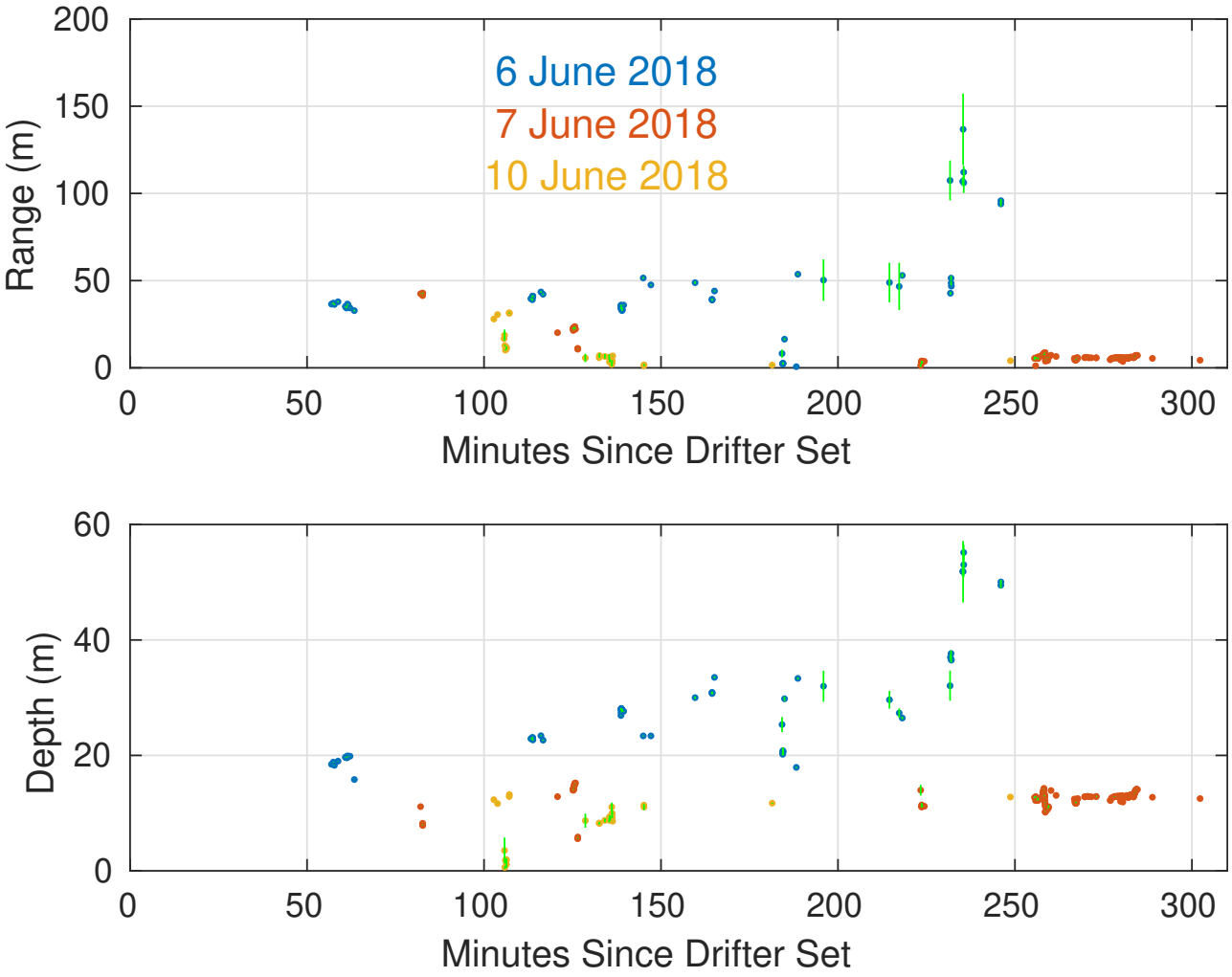

Figure 18: Range and depth of porpoises in Minas Passage/Channel obtained from a vertical array of four synchronized icListenHF hydrophones. Vertical bars are drawn in green to show plus/minus the standard error.

6 Long Term Drifter Tracking in Minas Passage

Interactions of marine animals with tidal turbines in the fast currents of Minas Passage involves two coordinate systems. First, the Eulerian coordinate system in which position is fixed with respect to the sea bed. For example, a turbine is installed at a fixed position to generate power from currents that vary with respect to time over the tidal cycle. Second, the Lagrangian coordinate system which is fixed to parcels of fluid that move with the current. Currents in Minas Channel and Minas Passage are much faster than the typical swimming speed of the marine animals found in the water column of that environment [20, 53, 54, 55, 56]. For this project we monitor porpoises as they live, which is to say in the Lagrangian coordinate system.

A model for animal-turbine interaction fails at the most fundamental conceptual level if it does not take both coordinate systems into proper account. To a first approximation, interaction operates as a Dirac delta function as animals pass near the turbine position and with far field consequences that are intrinsically tied to the wide ranging movement of animals that reside in the water column.

To date, most monitoring has been in the Eulerian coordinate system, using huge weights to hold moorings and platforms in the fast currents. Such moorings have turned out to be the most problematic factor for monitoring fish that have been implanted with acoustic tags [27], and flow noise makes porpoise monitoring problematic at certain times and locations [15, 16]. Motivated by these difficulties, we deployed instruments on drifters (Figure 19) in June 2017 to detect porpoises in Minas Channel/Passage [24]. In a separate spring 2017 project, Acadia University and the Gulf of Maine Institute (GOMI) released two surface drifters in Minas Channel. The GOMI/Acadia drifters reported position infrequently but those positions (Figure 19) — and trajectories of our instrumented drifter — lead us to hypothesise that trajectories can become trapped within a bounded zone that can be found at various stages of the tide in Minas Channel, Minas Passage and into Minas Basin. We hypothesize that these trajectories might be quasi-stable, in the sense that they may never exactly repeat themselves but that they remain within a bounded area for a long period of time.

Further support for quasi-stable tidal trajectories in Minas Channel/Passage/Basin can be inferred from an extensive accumulation of floating material that was first reported by Leim in 1931 [21, 22] and is commonly observed to this day [23]. This accumulation goes by a variety of local names. Presently, we shall call it the "Minas accumulation". The Minas accumulation is indicative of surface convergence in the tidal currents. Given plans that in-stream tidal turbines might one day be deployed from floating platforms in Minas Passage, there is good reason to measure the trajectory of the Minas accumulation and seek some understanding of both its formation and extent.

6.1 The Long Term Drifter (LTD)

A long term drifter (LTD) was constructed so that a trajectory within the Minas accumulation could be measured. Design elements expanded upon those of the near-surface GOMI drifters which used cross-vane drogues and a NOAA GPS-satellite tracking system. A plywood cross-vane drogue (four 1.22 m $\times$ 0.62 m panels) was suspended 4.5 m beneath the surface float (Figure 20). The NOAA GPS-satellite was placed within a watertight Maximum box that

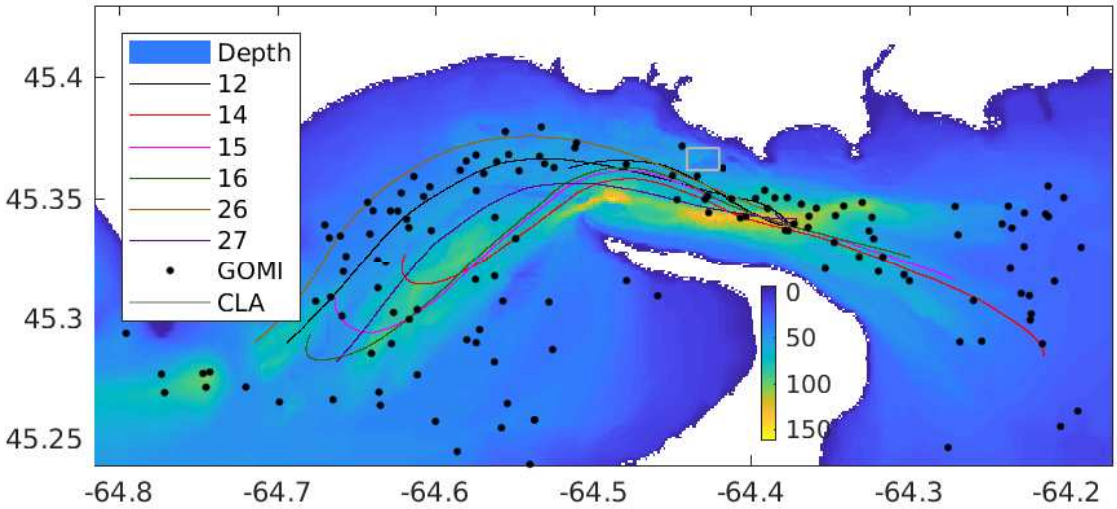

Figure 19: Lines show instrumented drifter tracks in June 2017. Positions of GOMI satellite-tracked GPS drifters are indicated with black dots. Bathymetry is indicated by the color, deep water being yellow and shallow blue. The FORCE Test Site (CLA) is plotted as a gray box.

was mounted at the top of the drifter pole. ABS pipe was used for the drifter pole with high density construction styrofoam (insulation) for flotation.

Satellite GPS positions were measured at 30 minute intervals but were not available for downloading from the website until several hours after measurement. Given the fast currents at our study area, the satellite GPS did not allow convenient recovery/servicing of the LTD when it was at sea. In order to be able to monitor the LTD position in real time, a Tractive GPS system was also included in the watertight Maximum box. The Tractive is a small device that is designed to fit on the collar of a dog. It uses 3G communications to transmit positions to a central website. Both the website and the Tractive can be accessed with a Smart Phone app. The Tractive has its own internal battery but extended operation requires a backup supply. To this end, a USB power pack was also included within the watertight Maximum box (Figure 20).

More frequent GPS position were obtained using a Columbus V-990 GPS Data Logger. The Columbus was powered by a stack of D-cells via an automobile 12 V-USB voltage regulator. Both the Colombus and power supply were contained within a separate ABS pipe with a Tee-fitting. The Tee-fitting (Figure 20) was painted white to prevent heating during sunny weather.

6.2 LTD measurements

A satellite-tracked drifter was deployed in Minas Passage on 11 June 2018. In the time since our proposal was written, an OERA-funded project has been initiated by Dr Michael Stokesbury to track acoustically-tagged fish in Minas Passage. It was deemed desirable to attach both a 69 kHz PPM Vemco acoustic tag and a 180/170 kHz PPM/HR Vemco tag in order to

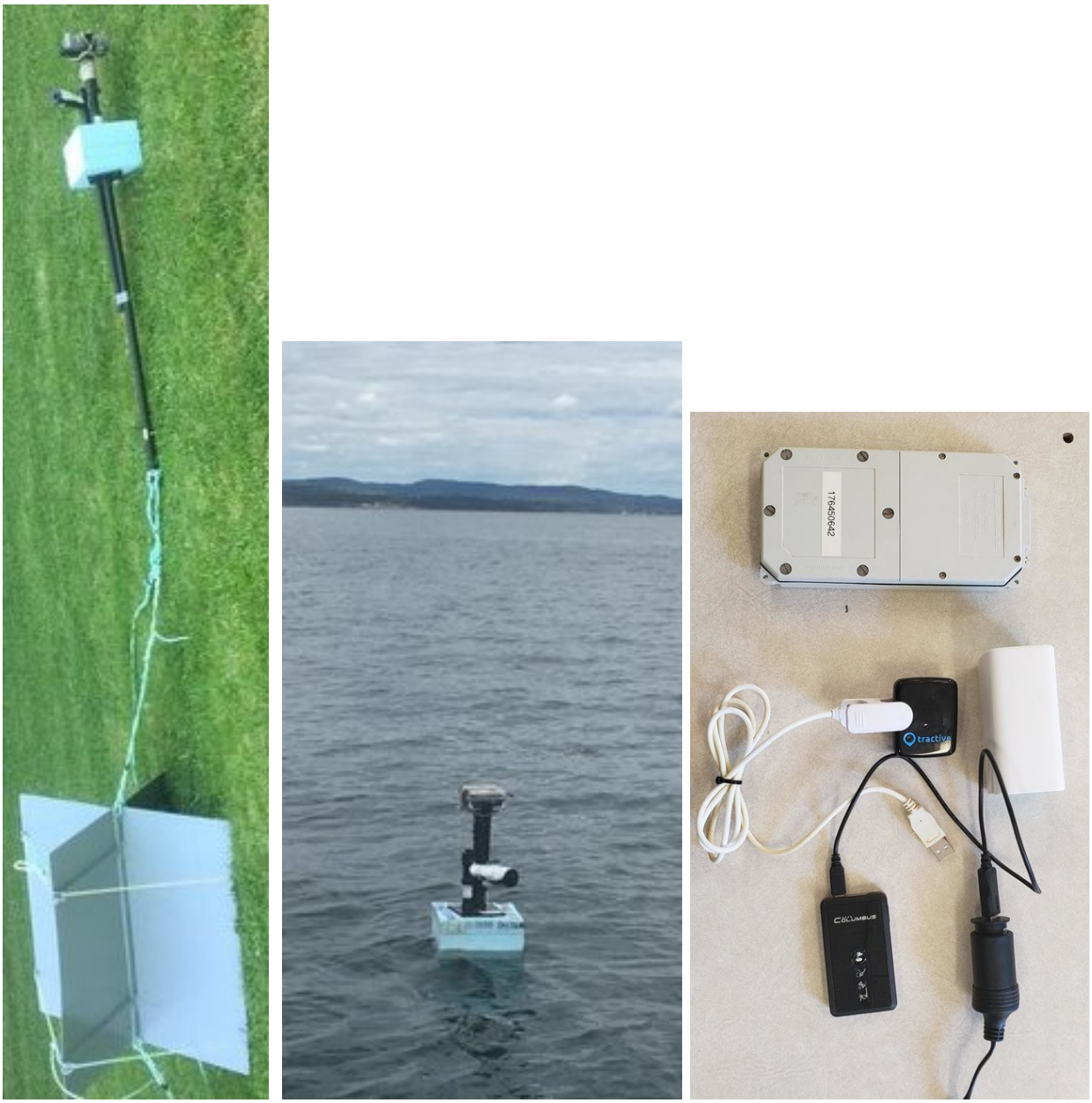

Figure 20: LEFT: Long Term Drifter (LTD) laid out on the grass. Note, the cross-vane drogue is hinged, for easy transport in the RHIB. Ropes tie it into the open-cross position just before deployment. MIDDLE: LTD deployed. A Maximum water-tight box on the top post contains the GPS-satellite transmitter and Tractive GPS/Smart Phone tracking system. The white paint is to prevent heating inside the black ABS fitting that houses the Columbus GPS Data Logger. RIGHT: From top to bottom; NOAA GPS-satellite transmitter, Tractive GPS/Smart Phone 3G real-time tracking system with USB power supply (white), Columbus V-990 GPS Data Logger with microSD Slot 4GB (50 million way-points) with USB connection to 12-Volt:USB-power adapter. The power adapter connects to a stack of D-cells.

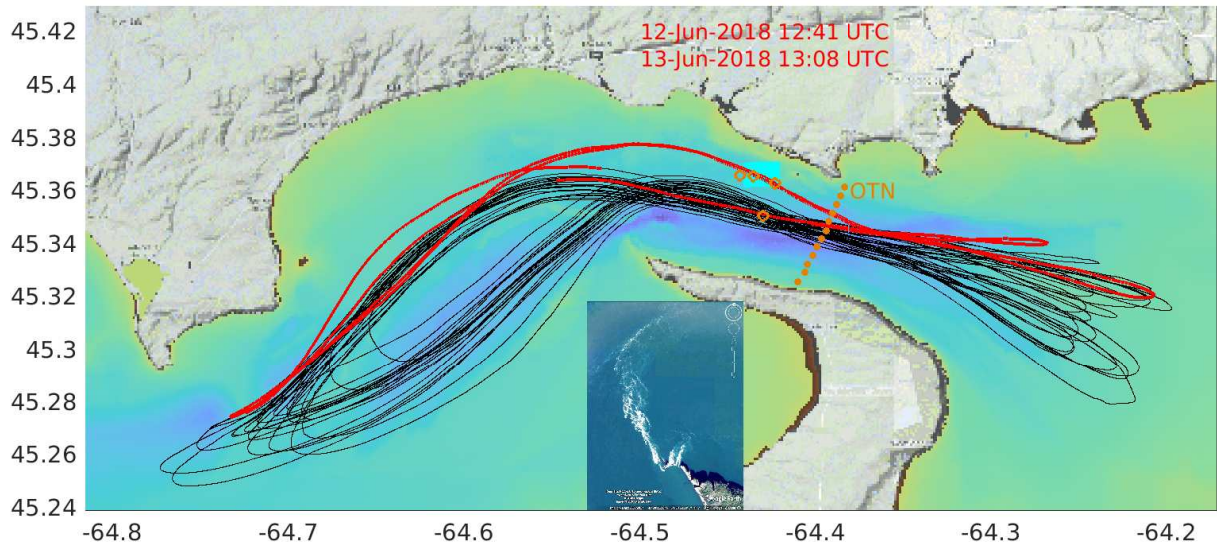

Figure 21: Drifter trajectory 11-23 June 2018. Red shows two tidal cycles when drifter trajectories went through the FORCE Crown Lease Area (cyan rectangle) on the flood tide. Open circles show positions at which Vemco receivers are moored on FORCE SUB floats. The Ocean Tracking Network (OTN) has Vemco receivers moored along the line shown by filled circles. A zoomed in GoogleEarth view has been inset and shows the cross-Passage jet that flows past Cape Split on the flood tide.

measure the effectiveness of receiver arrays installed in Minas Passage by Dr Stokesbury and by the Ocean Tracking Network (OTN). This prompted several further modifications to the drifter design from that which was originally proposed.

Whereas we had originally planned to attach two C-PODs, it was decided that this would be problematic because our work above (§4.3.3) demonstrated that the first harmonic of the 69 kHz tag would be incorrectly recorded by the C-POD as a porpoise. Satellite tracking has a maximum measurement rate of one position every 15 minutes. This was deemed too infrequent for detection-range testing of acoustically tagged fish, and would also have been too expensive. Nevertheless, the satellite tracking was kept as a fall back option, at a rate of one position fix every 30 minutes. A Columbus GPS-logger was attached to record position every second. Given that the drifter had to be recovered in order to download the GPS-logger, we also installed a 3G Tractive system so that we could navigate to the drifter at any time by using a smart-phone app. All in all, the new design had many desirable features compared to what was originally planned.

The drifter was recovered after 13 days. Our design would have allowed a month of tracking except that a water leak in the Maximum box damaged the battery that powered the Tractive. Nevertheless, a quasi-stable trajectory was obtained over most of a spring-neap tidal interval (Figure 21).

The LTD trajectory is coloured red for two tidal cycles (Figure 21), one on 12 June and the other on 13 June. During those tidal cycles the flood tide brought the LTD through the FORCE Test Site, along a trajectory that closely passed two of the FORCE SUB moorings upon which Dr Stokesbury had mounted Vemco VR2W and HR2 receivers. Sanderson et al.,

Figure 22: A large convergence zone indicates a large set of quasi-stable trajectories.

[57] have reported detections by receivers at the FORCE Test Site as the LTD passed by with its acoustic tags. There were many more passes over the OTN receiver line which spans Minas Passage but any detections by those Vemco receivers have not yet been analysed.

Our 2017 drifter-hydrophone measurements (Figure 19) showed ebb tide trajectories exiting Minas Passage like a jet which later bends gently with the coastline. The beginning of the flood tide trajectories showed a signature counterclockwise loop in Minas Channel (Figure 19) followed by a steep bend around Cape Split and into the middle of Minas Passage. Most of the LTD trajectories in Figure 21 also showed the jet-like, ebb-tide exit from Minas Passage followed by a counterclockwise loop in Minas Channel. The two exceptions to this rule were the two LTD drifter trajectories that passed through the FORCE Test Site on the flood tide. Those two trajectories returned into Minas Passage without making the wide counterclockwise loop in Minas Channel. We also note that the trajectories on the previous ebb tide were somewhat northward of most other ebb tide trajectories, as though they were on the northern edge of the ebb-tide jet.

This raises the question (which begs testing) of a more northern ebb-tide trajectory that might place drifters outside the quasi-stable trajectory and might eventually migrate onto the quasi-stable trajectory? The Minas accumulation (Figure 22) shows that surface drifters can be expected to converge into a zone that must be closely related to the quasi-stable trajectories. The extent of the Minas accumulation has not been measured and there are few high-resolution drifter tracks that illustrate how surface material converges there. There is one drifter track in Minas Channel that lays to the south of the quasi-stable trajectories. That trajectory is shown in a vimeo clip which is linked from a "going with the flow" Luna Ocean report to OERA [58]. The vimeo clip shows a Luna Ocean drifter deployed on the southern edge of Minas Passage during the outgoing tide exited to the south into Minas Channel. Details of the trajectory are not clearly reported but it is evident that the Luna Ocean drifter was swept into Minas Passage on some subsequent flood tide. This raises the question of the southern boundary of the region of quasi-stable trajectories and how (if) surface drifters might be entrained into the convergence zone from the south.

The western extent of LTD tidal excursions tended to be greater during spring tides (Figure 23 top panel). Ebb tide trajectories pass through the middle of Minas Passage where the water is deep and current speed is high. There is considerable flood/ebb asymmetry of drifter speed at both the western end of Minas Passage and also in Minas Channel (Figure 23, middle panel). The ebb tide exits Minas Passage as a jet. Notably, the core of this ebb tide jet travels at first in a nearly straight line from the deeper Minas Passage waters into a more

shallow part of Minas Channel. Given the barotropic nature of the tide, such flow over rising bathymetry might be expected to give rise to horizontal divergence and we observed much roiling motion during drifter-hydrophone experiments that passed through that location on the ebb tide.

The eastern limit of the LTD excursions was characterized more by variation in the longitudinal position (crosses in the upper panel of Figure 23). The LTD trajectory enters Minas Basin approaching high tide. At this time, the weakening tidal current does not force a jet into Minas Basin. Rather, LTD trajectories spread comensurate with the spreading bathymetric channels.

The top panel of Figure 23 also shows drifter positions at mid-tide which we define to be the halfway time between the eastern and western limits of each passage of the drifter. Average time between the western and eastern limits was 6.22 hours and is clearly related to the M2 and S2 tidal constituents. There is considerable variation in the mid-tide position on both the ebb (yellow) and flood (magenta).

The LTD might be roughly thought of as marking a water mass that flows back and forth through Minas Passage. Of course, this is not really correct if the trajectory depends upon a surface convergence because the water mass, unlike the LTD or flotsam, will not be constrained from moving in the vertical. Nevertheless, it is of interest to compare mid-tide positions of the drifter-hydrophone experiments with those of the LTD.

The drifter-hydrophone measurements did not always conveniently span the turn of the tide at both ebb and flood. We therefore defined the mid-tide time as being 3.11 hours before/after whichever turn of the tide was captured by the drifter-hydrophone trajectory. The lower panel of Figure 23 shows drifter-hydrophone trajectories measured in June 2017 (black lines) and June 2018 (orange lines). Ebb-tide drifts during June 2017 have mid-tide positions (yellow dots) that are sufficiently westwards as to indicate those measurements are made in a water mass that might be characterized as more "Minas Channel" than "Minas Passage". At the other extreme, we see that one of the flood-tide trajectories in June 2017 has a mid-tide position well to the east, indicative of the water mass having characteristics shifted towards those of "Minas Basin".

6.3 Dynamics of quasi-stable trajectories and convergence

We have not yet achieved a complete dynamical understanding of the quasi-stable trajectories and surface convergence that are indicated by drifter measurements and the long-observed "Minas accumulation" [21]. On the other hand, our observations do point to some salient mechanisms which likely contribute to such understanding.

Jet dynamics of the ebb current out of Minas Passage are of obvious importance. The classical concept would be that the ebb flow exits as a narrow jet of fast-flowing water into Minas Channel whereas there would be a broad flow in Minas Channel that approaches Minas Passage on the flood tide. LTD measurements support this notion (Figure 23). Presumably, water exiting Minas Passage earlier in the ebb tide might well pass sufficiently far beyond Cape Spencer so that broader, weaker flood currents cannot bring it back to Minas Passage. Perhaps this is a mechanism by which a portion of the floating material from the Minas accumulation might contribute to driftwood found at Driftwood Beach (Advocate Harbour)? Simulated trajectories from *accurate* hydrodynamic modelling and further drifter measurements might resolve this question. To date, the hydrodynamic models [11] use variable element geometric

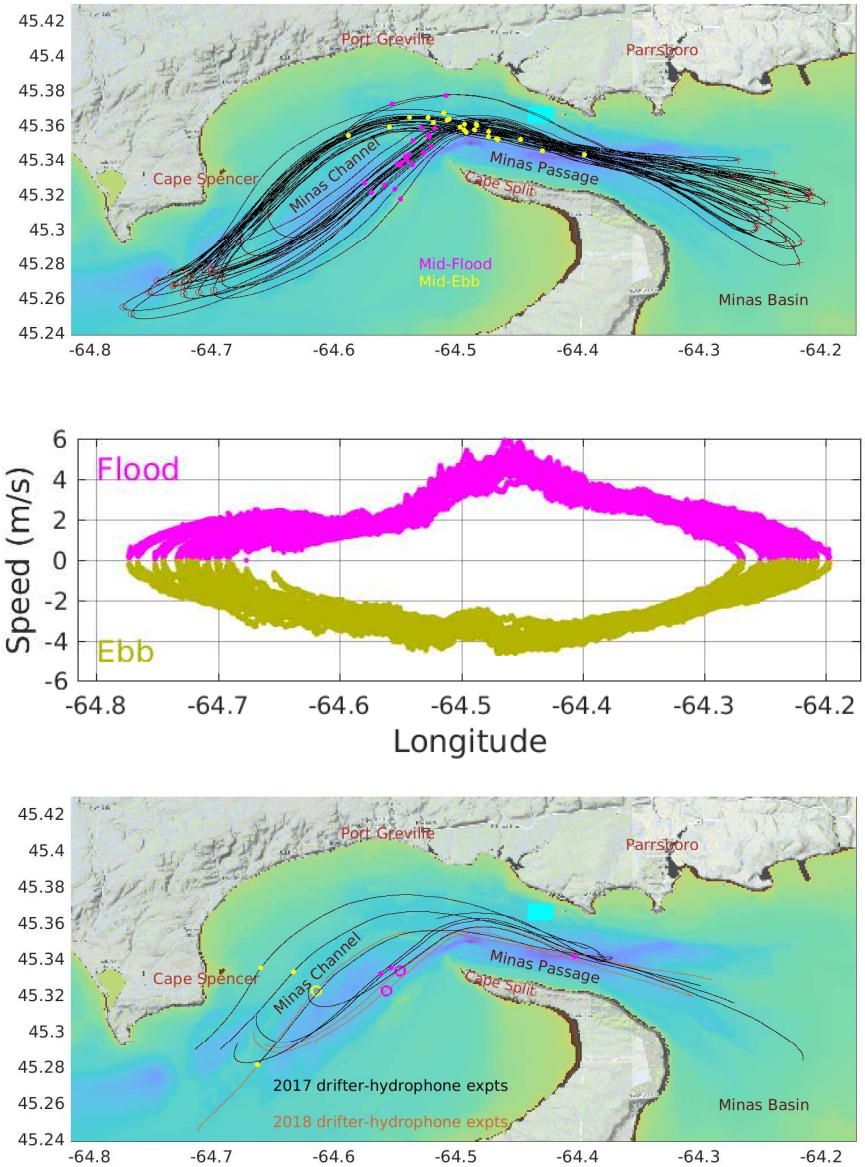

Figure 23: TOP: Drifter positions at turning points of the tide (red circles for low tide and red cross for high tide). Filled circles show drifter position at mid-tide (magenta for flood, yellow for ebb). MIDDLE: Drifter speed as a function of longitude. Bottom: Trajectories and mid-tide positions for drifter-hydrophone experiments. Mid-tide positions are shown using filled circles for June 2017 measurements and open circles for June 2018 measurements. Mid-tides are coloured yellow for ebb and magenta for flood.

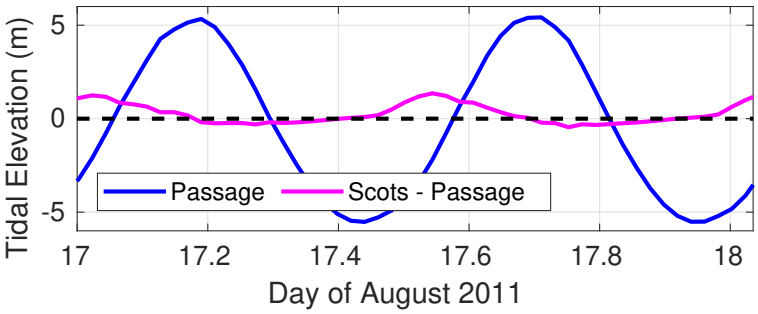

Figure 24: Modelled water level [11] in Minas Passage (blue) and water level in Scots Bay relative to that in Minas Passage (magenta).

methods that are optimized for boundary-fitting. These models have not been verified [59], have low-order truncation error, and propagating signals are aliased by variable grid scale. Such things matter little for modelling the tidal flow and water level because those dynamics are essentially one-dimensional and so a converged solution may be possible with a low-order model. High-order accuracy modelling is required [60] for accurate current modelling because the currents with which we are presently concerned have high dimensionality.

Currents in the vicinity of Cape Split are of particular interest. Figure 21 has a GoogleEarth image inset that shows white water associated with strong currents at Cape Split. These currents have a simple dynamical interpretation. Minas Passage represents a choke point for the tidal current, so water level both rises and falls faster on the seaward side. The hydrodynamic model [11] captures this mechanism well enough, as shown in Figure 24. On the flood tide, water level on the Scots Bay side of Cape Split is about 1 m higher than that on the Minas Passage side. This accounts for the broad inflow from Minas Channel to Minas Passage and the northwards sweep of drifter trajectories as they approach from Minas Channel.

Having been deflected northwards by the above cross-Passage gradient in hydrostatic pressure, the water (and drifters) flow into Minas Passage. The cross-Passage deflection is associated with a low pressure zone adjacent the southwestern shoreline of Minas Passage. An adverse boundary current is observed there. That adverse current is seen in computational results [11] but the low order computational accuracy of the model causes the simulated boundary eddy to be wider than observed.

A strong surface convergence must exist somewhere along the path taken by the LTD in order to explain the "Minas accumulation". A likely mechanism for such convergence may be associated with the above cross-Passage dynamical forcing. The problem has not yielded to analytical methods. Further progress will likely require very accurate computational modelling. In the meantime, for purposes of operating in-stream tidal turbines, it may be enough to know the extent of the "Minas accumulation" and how it moves.

Even though we only have the beginning of a dynamical understanding, it does suggest some things of a practical nature. For example, the jet outflow indicates that there should be a western limit to the "Minas accumulation" and also a westward limit to the set of quasi-stable trajectories. Similarly, the tentative relationship between cross-Passage water level gradient and convergence suggest an eastern limit to the "Minas accumulation" whereas the flow following spreading bathymetry into Minas Basin suggests an eastern limit to the set of quasi-stable trajectories. The extent of the "Minas accumulation" might be measured (visually or, perhaps, with radar) as it passes shore stations in Minas Passage.

Figure 25 shows three drifter experiments made at three different locations in three different years. Each set of tracks illustrates quite different characteristics.

1. The 2016 GOMI/Acadia trajectories (blue) on the south-eastern side of Minas Channel oscillate back and forth along a generally straight line for an entire month. There are a few small cross-channel displacements and two excursions westwards, approaching Isle Haute. GOMI/Acadia drifters were drogued very close to the surface (top 1 m) and would have suffered some displacement by winds. Nevertheless, all four drifters remained trapped within a generally rectilinear tidal excursion.

   We may think of the blue lines as marking a space-time zone where oscillating tidal currents are spatially uniform and that is associated with generally *stable, linear trajectories*. It is important to conceive of this zone in both space and time: the drifters being at the northeast end only near high tide and being at the southwest end only at low tide.

2. The 2018 LTD drifter track (black) is also stable but certainly not rectilinear with trajectories indicating strong spatio-temporal variations, strongly nonlinear dynamics, and strong convergence.

   We may think of the black lines as marking a space-time zone that has *stable, non-linear trajectories*. Again, it is important conceive of this zone as an area that shifts in time. Indeed, the black tracks begin where the blue tracks end but those beginnings and ends are at totally different times — so the two space-time zones are well and truly distinct.

3. The 2017 GOMI/Acadia drifters show positions of an entirely different character. These drifters were released near Isle Haute. Given the coastal geometry, one expects large spatial gradients in the currents in and around that area. Oscillating currents that have significant spatial variation are commonly associated with Lagrangian chaos. That is to say, the currents may be perfectly repeatable but trajectories of drifters that move with those currents are not.

   The 2017 GOMI/Acadia trajectories were deployed in a zone characterized by unstable trajectories. Being unstable, drifters did not remain there. Indeed, in due course both of the 2017 GOMI/Acadia drifters seem to have converged into the spatio-temporal zone of the LTD drifter which is characterized by convergence and stable, non-linear trajectories.

   Eventually the 2017 GOMI/Acadia drifters penetrated further into Minas Basin, perhaps driven by prevailing winds.

6.4 Drifters as measurement platforms

Moored measurement platforms have been very useful in Minas Passage [1, 18, 16, 27] but sometimes they have also been associated with issues that make measurements difficult to interpret [1, 16, 27] and sometimes even difficult to obtain [61].

The extended abstract that was presented at the MRC Research Forum [62] discusses the use of drifters as marine life monitoring platforms. In summary, three basic points are made:

1. For some types of measurement the drifter is a much less expensive measurement platform.

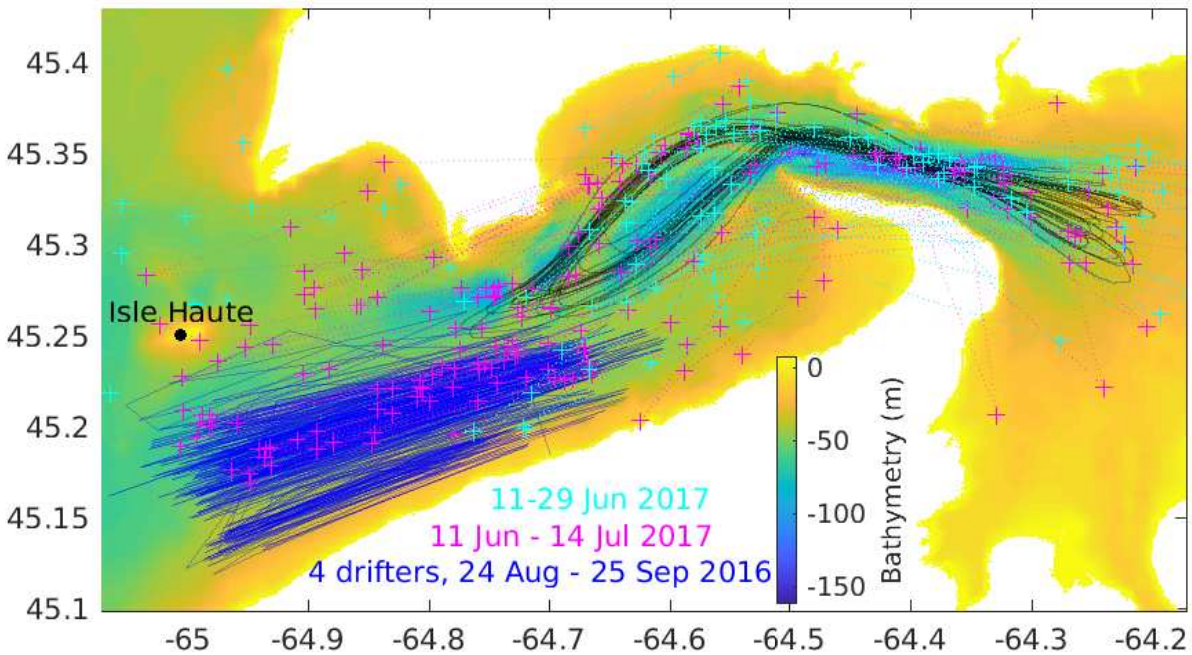

Figure 25: The edges of trajectory stability are suggested by three sets of drifter measurements. Blue dots show positions for four drifters released along a line of the southern side of Minas Channel by GOMI and Acadia University in 2016. Magenta and cyan crosses show positions of two drifters released near Isle Haute by GOMI and Acadia University in 2017. GOMI/Acadia drifters reported position at 4 hour intervals. The semi-transparent black lines show our 2018 LTD track.

2. Some phenomena are more reliably measured from a drifting platform, especially those that are sensitive to mooring motion and the effects of fast current relative to instrument sensors.

3. The drifting platform provides a perspective from the Lagrangian coordinate system, which is often closer to the framework in which animals live than the Eulerian coordinate system (ie fixed moorings), especially for animals that live in a fast-flowing marine environment. For example, our incidental measurements of an acoustically tagged fish (§4.4.4) demonstrated slow swimming speed relative to current. Imagine how much better the swimming speed could have been estimated with a drifter supporting an array of hydrophones from which the 3D position of the tagged fish could be obtained.

Further work to measure the extent of the convergence zone and more fully delineate quasi-stable trajectories would require deployment of many inexpensive drifters throughout that zone. We have already made a considerable effort to engineer our prototype drifter for a longer deployment for a future research project.

6.5 Recommendations for LTD design

A long term drifter (LTD) must overcome a number of human-caused hazards. In particular, mooring lines of lobster traps are ubiquitous along the edges of Minas Passage and to the east where Minas Passage opens up into Minas Basin. Obviously, the cross-vane drogue (Figure 20) might snag floating mooring lines. Similarly, any instruments suspended by ropes beneath the drifter might also become ensnared. Outside of lobster season, there remains the possibility of snagging ghost gear. Care is also required to avoid snagging floats that are used to mark locations within the FORCE Test Site.

It is necessary to construct the LTD so that it will not snag mooring lines. It turns out that this is not a particularly difficult thing to do if the surface float is made from a long tube (Figure 26) with all additional elements incorporated into a streamlined design along its length.

Our preliminary design was not ideal with regards to the configuration of the electronic components. As the GPS-satellite transmitter is robust, with its own internal power supply, it was not necessary to enclose it within the watertight Maximum box. In future, it could be bolted onto the top of the LTD as a stand-alone unit.

On the other hand, the watertight Maximum box was neither big enough nor sturdy enough to hold an adequate power supply for long term operation of the Tractive system. The new design (Figure 26) provides ample battery power and securely contains all electronics within a robust ABS tube.

There are two flotation options. First is the pole-float approach which makes buoyancy frequency substantially less than wind-wave frequency. That would be ideal for mounting hydrophones at the bottom of the tube, to minimize movement relative to the water. On the other hand, the pole-float approach may intermitently result in GPS electronics sometimes being below waterlevel when waves are too large. The second option is to clamp on a streamlined flotation collar so the buoyancy frequency is much higher than wind-wave frequency. That option is appropriate for attaching equipment that is not strongly sensitive to a little relative water motion. Similarly, depending upon measurement requirements, drag of the drifter can be increased by clamping tapered (vertically streamlined) fins to the pole.

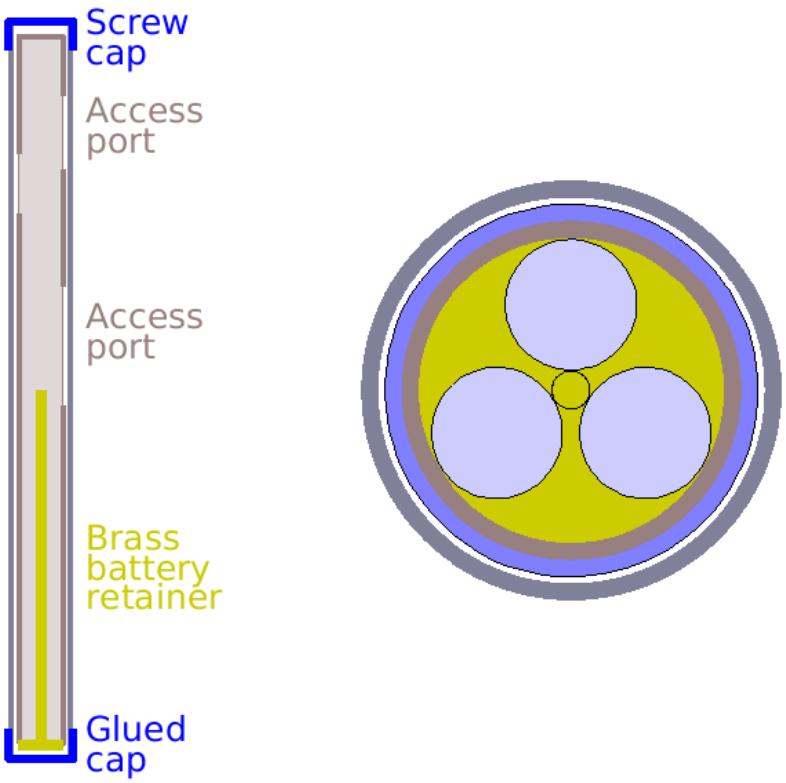

Figure 26: LEFT: Side view of the drifter housing tubes. A screw cap seals the top of the ABS outer housing (gray) and the glued end cap permanently seals the submerged part. The inner housing (brown) mounts electronics and batteries. Access ports are cut into the inner housing but otherwise it is a single PVC unit that slides into the outer housing. A brass plate threaded rod (yellow) retain the batteries. Access ports can be cut into the inner housing (brown), as required, in order to give access to the battery retainer and electronic components. Electronic components would be mounted, either directly or indirectly, onto the upper portion of the inner housing. The upper housing can be heat-shaped to suite mounting of electronics. RIGHT: Top view of drifter housing. Yellow shows the brass plate and rod. Three stacks of batteries are shown in light blue. A blue end cap (not shown in the side view) is wedged over the bottom of the inner housing (brown) so as to retain the brass plate. This end cap is taped onto the inner housing.

7 Going Forward: measurements using an LTD in 2019

Dr Stokesbury and his students have been collaborating with FORCE to detect acoustically-tagged sturgeon at the FORCE Test Site in Minas Passage. During summer 2018, detections were most frequent near low tide. On the other hand, detections of harbour porpoise vocalizations are more frequent at the FORCE Test Site near high tide [1, 14]. From a Lagrangian perspective, these observations indicate sturgeon that are generally resident within Minas Basin but move with the ebb tide into Minas Passage, and harbour porpoise which are more abundant in Minas Channel but move with the flood tide into Minas Passage.

There are uncertainties with both the measurements and the above interpretation. Moored instruments in Minas Passage are thought to have reduced detection efficiency when currents are fast. So the above measurements may have biases that are not fully understood or accounted for. Drifters provide one approach to obtain measurements that might avoid any confounding effects of flow noise (pseudo-sound) [17] and also enable observations to be obtained along paths that may approximate those of the animals.

In the 2019 field season, we intend to work with Dr Stokesbury and his students in order to detect sturgeon using the new LTD design. The idea is to mount an HR2 receiver to the base of the LTD. The LTD would be deployed at (or near) the FORCE Test Site at low tide. Detections of tagged sturgeon by HR2 receivers moored at the FORCE Test Site will then be compared with detections made by the HR2 receiver on the LTD. Perhaps the LTD measurements will provide a little more insight as to whether or not the detections at the FORCE Test Site are associated with tide assisted sturgeon movement. This will be a pilot experiment with the objective of testing the method.

8 Summary Points

These points are listed in the order that they appear in the main body of work.

- Visibility was higher than expected. Secchi disk depths were ≈ 4.25 m during neap tides and ≈ 2.75 m during spring tides. A GoPro camera identified a Secchi disk at 2.2 m range down to a depth of 20 m. See §4.1.

- C-PODs deployed on the 2017 drifter detected harbour porpoise vocalizations in 4% of minutes measured. A filtered Coda analysis of icListenHF hydrophones on the same drifter gave 19% detection positive minutes (FCI-DPM). See §4.3.1, §4.3.3. It is possible that the icListenHF detects porpoise vocalizations from a greater range, perhaps because the icListenHF has very high sensitivity, low self noise, and bandwidth that extends to higher frequencies than the C-POD.

- Timeseries of FCI-DPM are autocorrelated with an integral time scale of 4 minutes. See §4.3.1.

- FCI-DPM do not show any obvious trend to vary with location or hour of the day for measurements made from the drifter during daylight hours. See §4.3.1.

- Remarkably, the proportion of detection positive minutes (FCI-DPM) was essentially the same for icListenHF hydrophopnes on the 2017 drifter as it was for an icListenHF hydrophone mounted to a lander-platform at the FORCE Test Site in 2014. See §4.3.2

- The hydrophone on the lander-platform recorded fewer click trains per FCI-DPM, presumably because porpoises quickly pass by in the fast currents whereas hydrophones on the drifter move with the porpoises. See §4.3.2.
- Shorter inter-click intervals are more common at nighttime. See §4.3.2.
- CPOD-DPM are always associated with FCI-DPM. Many FCI-DPM have no associated CPOD-DPM even though there are visual sightings near that time. See §4.3.3
- There are clear relationships between FCI-DPM, CPOD-DPM and visual sightings. See §4.3.3.
- CPOD-DPM missed many (354) of the FCI-DPM. Scrutinizing detections suggests that this is not caused by the FCI obtaining false positives. Part of the problem is that C-PODs mounted to the drifter suffered lost measurement time when current speeds were greater than 1.5 m/s. See §4.3.3.
- The FCI-DPM missed only 28 of the CPOD-DPM. Examining timeseries indicated that sometimes weak porpoise clicks were rejected by FCI. CPOD-DPM included false positives that were caused by broadband spikes, a 118 kHz echo sounder, and the harmonic of a 69 kHz acoustic fish tag. See §4.3.3.
- A rigorous method is indicated for calculating: porpoise abundance, encounter with turbine, and avoidance of a tubine. See §4.4.
- Results suggest that during daylight hours the porpoises are as likely to be above 15 m depth as below. Reflections from the seasurface may bias this calculation towards underestimating the likelihood of porpoises being below 15 m. See §4.4.1.
- Probability that the same porpoise click is detected by two hydrophones separated by 2 m is about 0.7. This is less than would be theoretically expected at ranges greater than 24 m. Efforts to improve detection algorithms are the most profitable route for improving pair detection probability and for achieving detection of a signal by an array of many hydrophones in order to calculate the location of a vocalizing porpoise. See §4.4.2.
- Click trains sometimes appear to be a sequence of doublets. In that instance the second click of each doublet might be a reflection from the sea surface and it becomes possible to use two vertically-spaced hydrophones to calculate porpoise depth and range to the porpoise. See §4.4.3.
- Clicks are sometimes followed by what appears in a spectrogram to be a click that is smeared out with respect to time. These are bottom reflections and they can sometimes be used to obtain porpoise range and depth. See §4.4.3.
- Reflected paths are the logical equivalent of introducing virtual hydrophones and they can greatly increase the effective aperture of a hydrophone array. Our simulations suggest that this might vastly improve accuracy with which we can measure porpoise position. See §4.4.3.

- The drifting hydrophone array detected 180 kHz PPM signals from a fish tag. With the cooperation of the Ocean Tracking Network and DFO scientists, these were used to identify the tagged fish and crudely estimate swimming speed. See §4.4.4.

- A vertical array of 4 synchronized hydrophones was deployed on a pole-float drifter. During June 2018, measurements were made on 3 days. See §5). Preliminary analysis indicates that the proportion of detection positive minutes in June 2018 was similar to those in June 2017. See §5.3.

- Tilt measurements showed that the array was close to vertical most of the time but was sometimes tilted by strong tidal eddies. An association of tilt with increased ambient sound was noted. See §5.3.

- Preliminary analysis found porpoise at depths 0 to almost 60 m and ranges of a few metres from the hydrophones to about 100 m. See §5.3.

- Quasi-stable drifter trajectories were measured in the vicinity of Minas Passage. These trajectories extend from off Cape Spencer near low tide to the western side of Minas Basin near high tide. See §6.2.

- Quasi-stable drifter trajectories are associated with a zone of surface convergence that was first reported in 1931. See §6.2.

- The quasi-stable trajectories have highly nonlinear dynamics which are not completely understood by us. Clearly, tidal choking and associated cross-Passage pressure gradients at Cape Split play a role, as does the ebb-tide jet from Minas Passage. See §6.3.

- The southern side of Minas Channel has rectilinear tidal oscillations that support a space-time zone of stable, linear surface trajectories. See §6.3.

- Approaching Isle Haute, it seems that a zone of Lagrangian chaos is entered. Surface drifters beginning in that zone may migrate onto the space-time zone with quasi-stable drifter trajectories through Minas Passage. See §6.3.

9 Recommendations

1. The combination of icListenHF and the Coda software (developed by Acadia University and Ocean Sonics) resulted in more detections of harbour porpoise vocalizations than C-PODs that were co-deployed on a carefully designed drifter. A similar result was obtained when icListenHF hydrophones and C-PODs were co-deployed on a Lander platform at the FORCE Test Site [15, 16]. Our work cannot fully quantify the reasons for this but we can broadly identify two of them:

   - The icListenHF is a very sensitive instrument and has very low self noise. It also detects a wider range of frequencies than the C-POD. Our measurements and analyses (only some reported in this document) have convinced us that the quality of the hydrophone is an important factor for determining:
     - Precision with which vocalization detections are made, and
     - Maximum range from which vocalizations can be detected.
   - The algorithms used for detection are also important. Our most recent mathematical work demonstrates that more computationally expensive algorithms can be devised and that they work even better.

   Present work indicates that the above factors combine to degrade the detection performance of both instruments when ambient sound level is high in the fast currents of Minas Passage. But it must be emphasized that the C-POD performance suffers more than the icListenHF in this regard.

   Regardless of the above findings, the C-POD has been used to undertake many years of monitoring at and around the FORCE Test Site. The C-POD is a robust instrument that is convenient to deploy for long term monitoring. No instrument will work perfectly and our comparison of instruments shows that the C-POD detections are certainly associated with both icListenHF detections and visual observations.

   We recommend the C-POD as a useful and practicable instrument for detecting porpoise vocalizations for the purposes of long term monitoring of harbour porpoise activity patterns.

2. Measuring porpoise abundance and behaviour near in-stream turbines is necessary in order to address the requirements imposed by Canada's Fisheries Act [12].

   - **We recommend synchronized icListenHF hydrophones as an excellent option for resolving porpoise abundance, position, and behaviour near in-stream turbines. We also recommend ongoing efforts to improve:**
     - **Methods for deploying arrays of synchronized icListenHF hydrophones.**
     - **Methods and parallelized code for detecting harbour porpoise vocalizations in real time with high reliability from many instruments.**
     - **Methods for quickly and reliably converting the above detections into position. The basic mathematics is well known and already well coded. However, making it work in a complex and noisy environment still represents a significant challenge.**

We note that this work will naturally translate to measuring fish that carry acoustic tags.

- The C-POD is a very poor option for resolving porpoise abundance and position relative to an in-stream turbine. Long term monitoring with C-PODs can provide supporting evidence for the above but it is NOT sufficient in itself.

3. **We recommend expanded use of carefully designed drifters as measurement platforms in Minas Passage and neighbouring waters.** Many biological measurements are best made in the coordinate system of the water mass within which marine animals reside. Resolving the issues of animal-turbine interaction requires direct measurement as indicated above but such measurements need to be placed in the context of expanded biological knowledge. The drifter is the best platform for answering some biological questions.

4. SUB floats have long been recognized as having stability issues when used for mooring instruments in the fast-flowing waters of Minas Passage. **We recommend serious attention be given to either improving the SUB float or exploring alternative designs.**

10 Acknowledgements

Boat operation by Randy Corcoran was greatly appreciated and his expert porpoise spotting abilities contributed to the data set. We thank the Fundy Ocean Research Center for Energy (FORCE) for logistical support and for providing accommodation at Parrsboro. This project was supported by funding from OERA and a Mitacs internship awarded to Mike Adams. We thank Peter Porskamp, Jeremy Broome, and the Gulf of Maine Institute for their contributions to data collected in 2014, 2016 and 2017.

References

[1] Tollit, D., Joy, R., Wood, J., Redden, A., Booth, C., Boucher, T., Porskamp, P., & Oldreive, M. 2019. Baseline presence of and effects of tidal turbine installation and operations on harbor porpoise in Minas Passage, Bay of Fundy, Canada. Submitted to: Journal of Ocean Technology.

[2] May, R.M. 2010. Ecological science and tomorrows world. Philosphical Transactions of the Royal Society B 365, 41-47. doi:10.1098/rstb.2009.0164

[3] IPCC Fourth Assessment Report: Climate Change 2007

[4] McCormick, J. 1989. Acid Earth: The Global Threat of Acid Pollution (London: Earthscan, 1989)

[5] Dietrich, D.E., Bowman, M.J., Kolankiewicz, L., & Sanderson, B.G. 2017. Much Faster Sea Level Rising Ahead! J. Sustainable Energy Eng., 5(3): 207-211.

[6] The Shift Project. Data Source: The World Bank - World Development Indicators http://www.tsp-data-portal.org/Breakdown-of-Electricity-Generation-by-Energy-Source

[7] McCully, P. 2001. Silenced Rivers: The Ecology and Politics of Large Dams. Zed Books.

[8] Hawley, S. 2012. Recovering a Lost River: Removing Dams, Rewilding Salmon, Revitalizing Communities. Beacon Press.

[9] Lavin, M. F., Godinez, V. M., & Alvarez, L. G. 1998. Inverse-estuarine Features of the Upper Gulf of California. Estuarine, Coastal and Shelf Science 47, 769-795. https://doi.org/10.1006/ecss.1998.0387

[10] Dadswell, M.J., & Rulifson, R.A. 1994. Macrotidal estuaries: a region of collision between migratory marine animals and tidal power development. Biological Journal of the Linnean Society. 51, 93-113

[11] Karsten, R., McMillan, J., Lickley M., & Haynes R. 2008. Assessment of tidal current energy in the Minas Passage, Bay of Fundy. Journal of Power and Energy, Vol. 222 (A3), pp. 289-297.

[12] Fisheries Act, 1985, R.S., c. F-14, s. 1.

[13] Copping, A., Sather, N., Hanna, L., Whiting, J., Zydlewski, G., Staines, G., Gill, A., Hutchison, I., O'Hagan, A., Simas, T., Bald, J., Sparling, C., Wood, J., & Masden, E. 2016. Annex IV 2016 State of the Science Report: Environmental Effects of Marine Renewable Energy Development Around the World. pp 224.

[14] Wood, J., Tollit, D., Redden, A., Porskamp, P., Broome, J., Fogarty, L., Booth, C., & Karsten, R. 2013. Passive acoustic monitoring of cetacean activity patterns and movements in Minas Passage: Pre-turbine baseline conditions (2011-2012). Final Report for Fundy Ocean Research Center for Energy (FORCE) and Offshore Energy Research Association (OERA).

[15] Porskamp, P.H.J. 2015. Detecting and assessing trends in harbour porpoise (*Phocoena phocoena*) presence in and around the FORCE test site. Master's Thesis. Acadia University, Wolfville, NS.

[16] Porskamp, P.H.J., Broome, J.E., Sanderson, B.G., & Redden, A.M. 2015. Assessing the performance of two passive acoustic monitoring technologies for porpoise detection in a high flow tidal site. Journal of the Canadian Acoustical Association Vol. 43(3).

[17] Strasberg, M. 1979. Non-acoustic noise interference in measurements of infrasonic ambient noise, Journal of the Acoustical Society of America. Vol. 66. pp. 14871493. doi:10.1121/1.383543

[18] Adams, M.J., Sanderson, B.G., Porskamp, P., & Redden, A.M. 2018. Comparison of co-deployed drifting passive acoustic monitoring tools at a high flow tidal site: C-PODs and icListenHF hydrophones. Journal of Ocean Technology.

[19] Au, W.W.L, Kastelein, R.A., Rippa, T., & Schooneman, N.M. 1999. Transmission beam pattern and echolocation signals of a harbour porpoise (*Phocoena phocoena*). Journal of the Acoustical Society of America, Vol. 106 (6), pp. 3699-3705.

[20] Otani, S., Naito, Y., Kato, A., & Kawamura, K. 2000. Diving behavior and swimming speed of a free-ranging harbour porpoise, *Phocoena phocoena*. Marine Mammal Science, Vol. 16(4), pp. 811-814.

[21] Leim, A.H. 1931. The fauna of Minas Channel, Minas Basin and the Shubenacadie River.

[22] Bousfield, E.L., & Leim, A.H. 1958. The Fauna of Minas Basin and Minas Channel. Bulletin No. 166, National Museum of Canada, Contributions to Zoology.

[23] FORCE 2009. Environmental Assessment Registration Document — Fundy Tidal Energy Demonstration Project, Volume I: Environmental Assessment.

[24] Adams, M.J. 2018. Application of a Multi-Hydrophone Drifter and Porpoise Detection Software for Monitoring Atlantic Harbour Porpoise (*Phocoena phocoena*) Activity in and near Minas Passage. B.Sc. Honours Thesis, Biology, Acadia University, Wolfville, N.S.

[25] Adams, M.J., Redden, A.M., Sanderson, B.G. 2018. Passive Acoustic Drift Surveys of Harbour Porpoise (*Phocoena phocoena*) Presence and Behaviour in the Minas Passage and Adjacent Waters. BoFEP Conference, Truro.

[26] Sanderson, B.G., & Adams, M.J. 2018. Range and Depth from Reflected Porpoise Clicks. Research notes.

[27] Sanderson, B., Buhariwalla, C., Adams, M.J., Broome, J., Stokesbury, M., & Redden, A.M. 2017. Quantifying detection range of acoustic tags for probability of fish encountering MHK devices. European Wave and Tidal Energy (EWTEC) 2017 Conference. Cork, Ireland. pp. 10

[28] Villadsgaard, A., Wahlberg, M., & Tougaard, J. 2007. Echolocation signals of wild harbour porpoises, *Phocoena phocoena*. Journal of Experimental Biology, 210: 56-64.

[29] Press, W.H., Flannery, B.P., Teukolsky, S.A., & Vetterling, W.T. 1986. Numerical Recipies, The Art of Scientific Computing. Cambridge University Press, Cambridge, 818 pp.

[30] Hinze, J.O. 1975. Turbulence. McGraw-Hill, Inc. pp. 790.

[31] Wahlberg, M., Linnenschmidt, M., Madsen, P., Wisniewska, D., & Miller, L. 2015. The Acoustic World of Harbor Porpoises, American Scientist, 103 (1): 46 DOI: 10.1511/2015.112.46

[32] Sorensen, P.M., Wisiewska, D.M., Jensen, F.H., Johnson, M., Teilmann, J., & Madsen P.T. 2018. Click communication in wild harbour porpoises (*Phocoena phocoena*). Nature, 8:9702. DOI:10.1038/s41598-018-28022-8

[33] Clausen, K. T., Wahlberg, M., Beedholm, K., Deruiter, S., & Madsen, P. T. 2010. Click communication in harbour porpoises (*Phocoena phocoena*). Bioacoustics 20, 1-28.

[34] Sarnocinska, J., Tougaard, J., Johnson, M., Madsen, P. T., & Wahlberg, M. 2016. Comparing the performance of C-PODs and SoundTrap/PAMGUARD in detecting the acoustic activity of harbor porpoises (*Phocoena phocoena*) Presented at the Fourth International Conference on the Effects of Noise on Aquatic Life, Dublin, Ireland. doi:10.1121/2.0000288

[35] Jacobson, E.K., Merkens, K.P.B., Forney, K.A., & Barlow, J. 2017. Comparison of harbor porpoise(*Phocoena phocoena*)echolocation clicks recorded simultaneously on two passive acoustic monitoring instruments. U.S. Department of Commerce, NOAA Technical Memorandum NOAA-TM-NMFS-SWFSC-583. doi: 10.7289/V5/TM-SWFSC

[36] Clausen, K.T., Tougaard, J., Carstensen, J., Delefosse, M., & Teilmann, J. 2018. Noise affects porpoise click detections — the magnitude of the effect depends on logger type and detection filter settings. Bioacoustics. doi:10.1080/09524622.2018.1477071

[37] Hansen, S. 2011. Assessing acoustic and visual monitoring techniques for the conservation management of bottlenose dolphins (*Tursiops truncatus*) in a special area of conservation. Master's thesis, Galway Mayo Institute of Technology.

[38] Roberts, B.L., & Read, A.J. 2014. Field assessment of C-POD performance in detecting echolocation click trains of bottlenose dolphins (*Tursiops truncatus*). Marine Mammal Science Vol. 31(1) pp. 169-190. doi: 10.1111/mms.12146

[39] Palka, D. 1996. Effects of Beaufort sea state on the sightability of harbor porpoises in the Gulf of Maine. Report of the International Whaling Commission Vol. 46 pp. 575582.

[40] Sanderson, B.G., Adams, M.J., & Redden, A.M. 2018. Using reflected clicks to Monitor range and depth of porpoise. Extended abstract submitted to: Proceedings of the 2018 Marine Renewables Canada Research Forum Halifax, Canada, November 20, 2018.

[41] Fisher F.H., & Simmons V.P. 1977. Sound absorption in seawater. Journal of the Acoustical Society of America, Vol. 62, pp. 558-564.

[42] Laplanche, C., Olivier, A., Lopatka, M., & Motsch, J-F. 2005. Male sperm whale acoustic behavior observed from multipaths at a single hydrophone. The Journal of the Acoustical Society of America (JASA), 118. pp. 2677-2687. ISSN 0001-4966

[43] Macaulay, J., Gordon, J., Gillespie, D., Malinka, C., & Northridge, S. 2017. Passive acoustic methods for fine-scale tracking of harbour porpoises in tidal rapids. The Journal of the Acoustical Society of America, Vol. 141, pp. 1120. doi: 10.1121/1.4976077 https://doi.org/10.1121/1.4976077

[44] Sanderson, B.G., 2017. Acoustic Positioning Finding. P&I Tier II report to Ocean Sonics.

[45] Sanderson, B.G., Adams, M.J., & Redden, A.M. 2018. Tag Detected by Drifting icListen. Research notes.

[46] LeBlond P.H., & Mysak L.A. 1978. Waves in the Ocean. Elsevier Oceanography Series 20. Elsevier, Amsterdam, Oxford, New York.

[47] Neumann, G., & Pierson, W.J. Jr. 1966. Principles of Physical Oceanography. Prentice-Hall, Inc. Englewood Cliffs, N.J.

[48] Sanderson, B.G. 2017. Drifter Design for Hydrophone Measurements. IRAP Report to OceanSonics.

[49] Lossent, J., Lejart, M., Folegot, T., Clorennec, D., Di Iorio, L., & Gervaise, C. 2018. Underwater operational noise level emitted by a tidal current turbine and its potential impact on marine fauna. Marine Pollution Bulletin, Vol. 130,pp. 323-334

[50] Wisniewska, D.M., Johnson, M., Teilmann, J., Siebert, U., Galatius, A., Dietz, R., & Madsen, P.T. 2018. High rates of vessel noise disrupt foraging in wild harbour porpoises (*Phocoena phocoena*). Proceedings of the Royal Society B, Vol. 285: 0172314. https://doi.org/10.1098/rspb.2017.2314

[51] Mikkelsen, L., Hermannsen, L., Beedholm, K., Madsen, P.T., & Tougaard J. 2017. Simulated seal scarer sounds scare porpoises, but not seals: species-specific responses to 12kHz deterrence sounds. Royal Society Open Science. Vol. 4(7). doi: 10.1098/rsos.170286

[52] Teilmann, J., Henriksen, O., Carstensen, J., & Skov, H. 2002. Monitoring effects of offshore windfarms on harbour porpoises using PODs (porpoise detectors). Report to Ministry of the Environment, Denmark.

[53] Sambilay, V.C. Jr., 1990. Interrelationships between swimming speed, caudal fin aspect ratio and body length of fishes. Fishbyte 8(3):16-20.

[54] Castro-Santos, T.R. 2002. Swimming Performance of Upstream Migrant Fishes: New Methods, New Perspectives. Ph.D. Dissertation, University of Massachusetts Amherst. 185 pp.

[55] Aleyev, Y.G. 1977. Nekton, Dr. W. Junk b.v., The Hague 1977, Translated from Russian by B. M. Meerovich.

[56] Haro, A., Castro-Santos, T., Norieka, J., & Odeh, M. 2004. Swimming performance of upstream migrant fishes in open-channel flow: a new approach to predicting passage through velocity barriers. Can. J. Fish. Aquat. Sci. 61:1590-1601.

[57] Sanderson, B.G., Adams, M.J., & Stokesbury, M. 2018. Interim Report: Detection Range Testing in Minas Passage, June 2018.

[58] Luna Ocean, 2018. Going With the Flow 2: Use of drifters to address uncertainties in the spatial variability of tidal flows. Final Report to OERA. See video clip: https://vimeo.com/224721952

[59] Roache, P.J. 2009. Fundamentals os Verification and Validation. Hermosa Publishers, New Mexico, USA.

[60] Sanderson, B.G. 1998. Order and resolution for computational ocean dynamics. J. Phys. Oceanogr. 28: 1271-1286.

[61] Ocean Sonics. 2018. Data Analysis Report. A report by Ocean Sonics Ltd to Cape Sharp Tidal regarding the Environmental Effects Monitoring Program.

[62] Sanderson, B.G., Adams, M.J., & Redden, A.M. 2018. Quasi-stable drifter trajectories in the Minas Channel-Passage-Basin enable efficient monitoring in the coordinate system of marine animals. Extended abstract submitted to: Proceedings of the 2018 Marine Renewables Canada Research Forum Halifax, Canada, November 20, 2018. Extended abstract submitted to: Proceedings of the 2018 Marine Renewables Canada Research Forum Halifax, Canada, November 20, 2018.